

AD-A050 606

OBSERVATORIO DEL EBRO TORTOSA (SPAIN) IONOSPHERIC SECTION F/G 4/1
IONOSPHERIC ELECTRON PRODUCTION RATE FOR GRAZING INCIDENCE AT T--ETC(U)
DEC 77 L F ALBERCA

AFOSR-75-2745

UNCLASSIFIED

AFGL-TR-78-0044

NL

| OF |

AD-A050606



END
DATE
FILMED
4 -78
DDC

AFGL-TR-78-0044

AD A 050606

AD No. _____
DDC FILE COPY

①

SCIENTIFIC REPORT N.º 6

IONOSPHERIC ELECTRON PRODUCTION RATE FOR
GRAZING INCIDENCE AT THE EBRO OBSERVATORY

LUIS F. ALBERCA, S. I.

OBSERVATORIO DEL EBRO
IONOSPHERIC SECTION
ROQUETAS (TARRAGONA)
SPAIN

DDC
RECEIVED
MAR 2 1978
D

404598

DISTRIBUTION STATEMENT A

Approved for public release;
Distribution Unlimited

AFGL-TR-78-0044

GRANT N° AFOSR 75-2745

29 December 1977

Final Report

IONOSPHERIC ELECTRON PRODUCTION RATE FOR
GRAZING INCIDENCE AT THE EBRO OBSERVATORY

L. F. Alberca, s.I.

ACCESSION FOR	
DTIC	White Section <input checked="" type="checkbox"/>
DDC	Ref Section <input type="checkbox"/>
UNANNOUNCED	<input type="checkbox"/>
JUSTIFICATION	
BY	
DISTRIBUTION/AVAILABILITY CODES	
SIGL	AVAIL. 800/ or SPECIAL
A	

OBSERVATORIO DEL EBRO
IONOSPHERIC SECTION
ROQUETAS
(TARRAGONA) Spain

DDC
RECEIVED
MAR 2 1978
D

THE RESEARCH REPORTED IN THIS DOCUMENT HAS BEEN SPONSORED
IN PART BY THE AIR FORCE CAMBRIDGE RESEARCH LABORATORIES
THROUGH THE EUROPEAN OFFICE OF AEROSPACE RESEARCH OAR
UNITED STATES AIR FORCES.

DISTRIBUTION STATEMENT A

Approved for public release;
Distribution Unlimited

ABSTRACT

Values of total electron content of the ionosphere, obtained at the Observatorio del Ebro by the Faraday rotation method, have been analyzed to study electron production rates. Daily values of the electron production rate, integrated with respect to height through the ionosphere, were determined at sunrise for the period August 1973 - July 1974, by a method that makes use of a two components model atmosphere. A Fourier analysis of the results indicates an annual and a semianual variation of the production rate values. A comparison with results of other authors seems to indicate a latitudinal dependence of the semiannual variation; no similar effect was found for the annual variation.

INDEX

1.	<u>INTRODUCTION</u>	1
2.	<u>METHOD OF ANALYSIS</u>	2
2.1	THE CONTINUITY EQUATION	2
2.2	NEUTRAL ATMOSPHERE	3
2.3	PHOTOIONIZATION	8
2.4	GRAZING INCIDENCE	10
2.4.1	<u>Absorption of radiation</u>	10
2.4.2	<u>Production rate</u>	15
2.5	IONIZATION LOSS RATE	18
2.6	TOTAL ELECTRON CONTENT VARIATION	22
2.7	INTEGRATED PRODUCTION RATE FOR $\chi = 90^\circ$	25
3.	<u>RESULTS</u>	26
3.1	VALUES AT OBSERVATORIO DEL EBRO	26
3.2	COMPARISON WITH OTHER AUTHORS	30
3.2.1	<u>Mean value</u>	30
3.2.2	Annual and semiannual variation	34
3.3	DISCUSSION	38
4.	CONCLUSIONS	42
	APPENDIX	45
	TABLES	47
	BIBLIOGRAPHY	59

1. INTRODUCTION.

In a previous report (Alberca and Galdón, 1974) we gave results of total electron content of the ionosphere for a period of six months. The data were derived every 2,5 minutes from the signal of the geostationary satellite INTELSAT II-F3 by the Faraday rotation method. An analysis similar to the one described by Garriot and Smith (1965), was applied to the sunrise period data in order to obtain daily values of the integrated ionization rate of the ionosphere for an overhead sun.

In the present work we use a more sophisticated method to obtain more accurate values of the integrated ionization production rate for a zenithal angle of the sun of 90° , (Q_{90}). In the following sections we describe the method of analysis, in which a two component model of the neutral atmosphere has been incorporated. The model, whose description is given in 2.2, is used in 2.3 and 2.4 to obtain an expression for the photoionization rate for grazing incidence. An expression for the ionization loss rate is also obtained in 2.5. The formulae obtained in these paragraphs are used in 2.6 to obtain the theoretical total electron content given by the model for the sunrise period. The part 2.7 contains the method to obtain the integrated ionization production rate by comparing the theoretical and the experimental data of the total electron content. We give in section 3 the results of the production rate found at the Observatorio del Ebro by the application of the method described. Its mean value as well as its seasonal va-

riations are compared with the results of other authors and its implications are discussed. Finally, section 4 contains the conclusions drawn from the previous discussion.

2. METHOD OF ANALYSIS.

2.1 THE CONTINUITY EQUATION.

The determination of Q90 is done by comparing the experimental data of total electron content (TEC) deduced through the Faraday rotation method for the sunrise period, to the theoretical values, deduced from a model of the ionosphere, at the same period.

The model is based on the well-known continuity equation for electrons:

$$\frac{\partial N}{\partial t} = q - l - \nabla \cdot (Nv) \quad (1)$$

where q and l are respectively the production and loss rate, N the electron density and v the drift velocity of the ionization, produced by all the different forces.

This equation is valid at any height, z , of the ionosphere, so that it can be integrated over all heights. Before doing it, we assume that only vertical derivatives contribute to the value of the divergence. Then, the divergence term can be neglected when integrated over all heights. This is equivalent to assume that the T.E.C. is not modified by changes in the electronic profile, due to vertical movements of ionization. In the real ionosphere, vertical movements of ionization do have an indirect effect on the electron content, because the loss coefficient

diminishes with increasing heights. Nevertheless, this effect is very small at sunrise conditions, first of all because the loss itself is very small, and secondly because, due to the rapid increase of the electron content during this period, most of the ionization present at a given time, has been produced little time before. If the movement is not very fast, the displacement of this ionization should not be big enough to produce appreciable changes on the loss rate. In fact, at middle latitudes, at sunrise, only an E-W movement of ionization could affect substantially the total electron content, because of the strong gradient of electron density in that direction at that period. But, unless there are strong electric fields, that we do not expect, this movement is impeded by the geomagnetic field, whose direction lays on a plane almost perpendicular to the E-W direction. The integration of the two members of the equation (1) with the conditions just assumed gives

$$\frac{dN_T}{dt} = Q - P \quad (2)$$

Where N_T is the total electron content, and Q and P , respectively the integrated production and loss rate.

2.2 NEUTRAL ATMOSPHERE.

The two terms of the second member of equation (2) depend very strongly on the properties of the neutral atmosphere that receives the ionizing radiation. To solve equation (2) is then necessary, to establish a model of neutral atmosphere from which expressions for the different terms can be deduced.

The model we have adopted is an approximation of that of Jacchia (1971). We have found some relatively simple formulae that give a representation of the neutral atmosphere, similar to the Jacchia model for the same boundary conditions. The formulae are valid for an exospheric temperature range at least between about 700° K and 1000° K that corresponds to the temperature variation during the considered period. The lower limit of validity of the model proposed is $Z_0 = 120\text{Km}$. The temperature at this level is not kept constant as in other models. On the contrary, we make it dependent of the exospheric temperature, in order to obtain a better fitting to the experimental data.

A list of the variables that are used on the formulae is given below:

- m = molecular weight
- K = Boltzman constant
- T_∞ = exospheric temperature
- T = temperature at height z
- T_0 = temperature at height z_0 (depends on T_∞)
- g = gravitational acceleration
- $n(X)$ = numerical density of the X component at height z
- $n_0(X)$ = numerical density of the X component at height z_0 (depends on T_∞)
- C = constant = 910
- b = parameter (depends on T_∞)
- k = parameter (depends on T_∞ and on m)
- s = parameter (depends on T_∞ and on m)

All the variables, as well as the temperature and density at the Z_0 level, can be obtained from the exospheric temperature, T_∞ , through the formulae given in Ap

pendix.

The exospheric temperature, depends on the solar radiation and the geomagnetic activity, and the method to calculate it is the same as in the Jacchia model.

The temperature distribution with height is given by the equation

$$T = T_{\infty} - (T_{\infty} - T_0)e^{-b(z-z_0)} \quad (3)$$

were $z_0 = 120\text{Km}$. T_0 and b depend on T and are obtained through the equations given in Appendix.

In fig. 1 a comparison between the temperature distribution given by (3) and the Jacchia (1971) model is given for two different exospheric temperatures. As can be seen, in both cases the curves are very similar.

We assume the neutral atmosphere to be composed by three elements, O, O_2, N_2 . Later on we shall see that the contribution of O_2 to the total electron content variation is really negligible so that only O and N_2 shall be taken into account in the analysis of the data, nevertheless, in this part, the three elements are considered.

We assume, as usual, that the three elements are in diffusive equilibrium, so that the density distribution with height, z , of each component is given by

$$n = n_0 (T_0/T) e^{-(m/K) \int_{z_0}^z g/T dz} \quad (4)$$

To obtain an expression of the integral that appears in the exponential, we approximate the relation g/T through the sum

$$g/T = C/T + f(z-z_0) \quad (5)$$

where C is a constant and $f(z - z_0)$ a function whose integral is:

$$\int_{z_0}^z f(z-z_0) dz = \ln \left[F(z-z_0) \right]^{-K/m} \quad (6)$$

with

$$F(z-z_0) = 1 + k(z-z_0) e^{s(z-z_0)} \quad (7)$$

where, as has been indicated, k and s are two parameters that can be obtained from T_{∞} through the formulae of Appendix.

With these approximations, the integral of eq. 4 becomes

$$\int_{z_0}^z g/T dz = C/(bT_{\infty}) \ln(T/T_{\infty}) + \ln(F(z-z_0))^{-K/m}$$

and the density

$$n = n_0 \cdot \frac{(1 + \frac{mC}{bKT_{\infty}})^{-\frac{1}{bKT_{\infty}}}}{1 + \frac{mC}{bKT_{\infty}}} e^{-\frac{mC}{KT_{\infty}}(z-z_0)} F(z-z_0) \quad (8)$$

We put

$$H_{\infty} = \frac{KT_{\infty}}{mC} \quad (9)$$

that has the form of a scale height of temperature T_{∞} and acceleration of gravity equal to C .

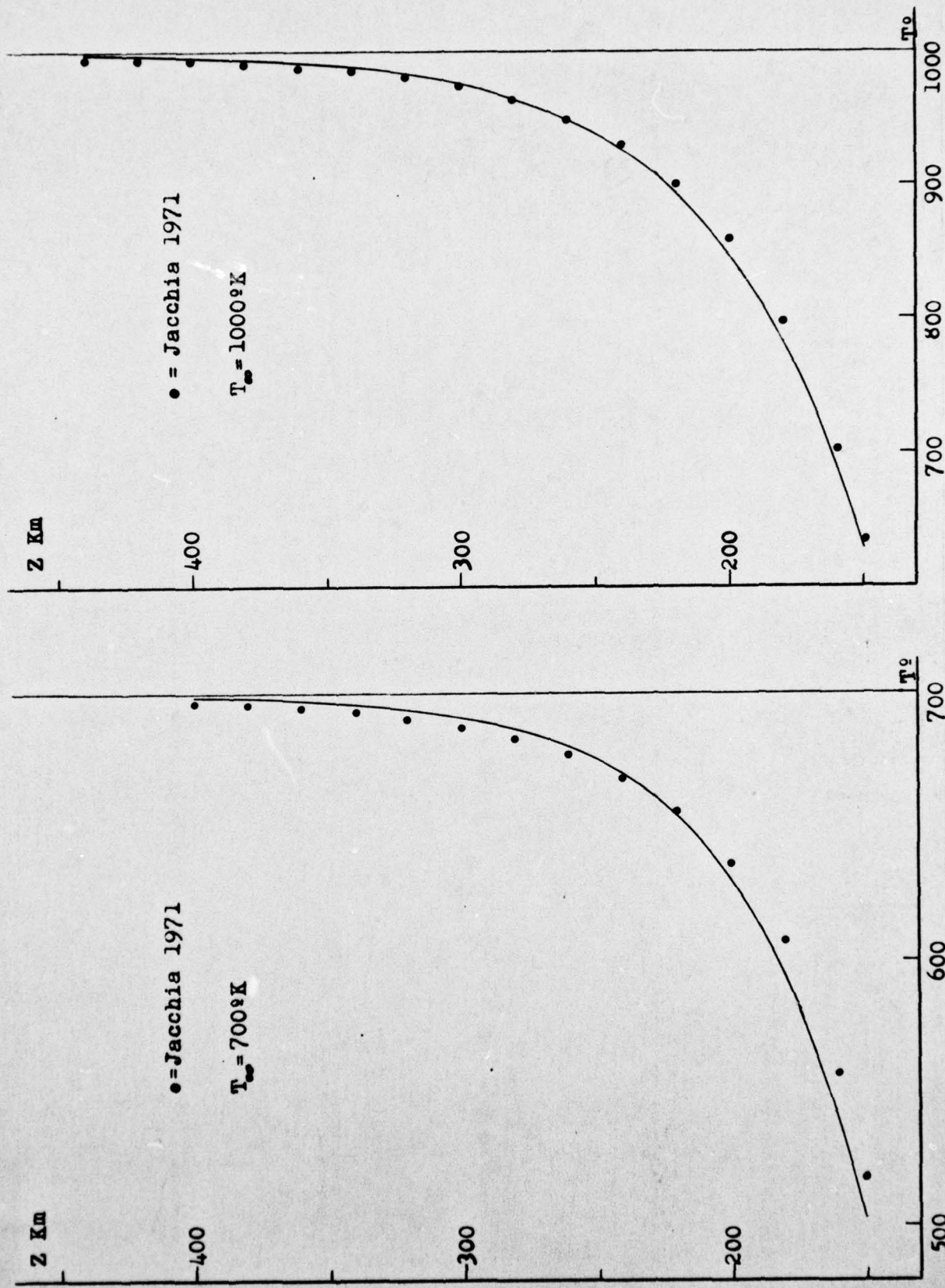


fig. 1.- Temperature profiles of the neutral atmosphere and its comparison with Jacchia's (1971) model

If we call

$$\gamma = 1 + \frac{1}{bH_{\infty}} \quad (10)$$

and substitute $F(z - z_0)$ by its expression(t), the equation 8 becomes

$$n = n_0 \left[\frac{I_0}{T} \right]^{\gamma} e^{-\frac{1}{H_{\infty}}(z-z_0)} (1+k(z-z_0)e^{s(z-z_0)}) \quad (11)$$

with T given by (4).

In Tables I we give the values of $\log n$ for the three components, obtained by eq. 11 for different exospheric temperatures. Also the corresponding values of the Jacchia (1971) model and the relative difference between both models are shown. As can be seen the differences between the models are not greater than 2% till very high altitudes, and they are greater than 10% only in regions where the density is less than 20cm. The contribution of this region to the total ionization of the ionosphere is so small that, even if the errors in the determination of the density of the components are very high, the results are not affected.

2.3 PHOTOIONIZATION.

As it is well known, most of the free electrons in the middle latitude ionosphere, are produced by photoionization.

In a mixture of gases, the photoionization rate of each component, q_j , produced by a monochromatic radiation of flux ϕ is given by

$$q_j = \Phi_{\bullet} \sigma_{ij} n_j e^{-\sum_l \sigma_{al} \int_s n_l ds} \quad (12)$$

where σ_{ij} and σ_{aj} are respectively the ionization and absorption cross sections of the j component and n_j the numerical density. The sum \sum_l is extended to all the components and the integral is taken along the ray path.

Since the ionizing radiation of the atmosphere is not monochromatic, eq. 12 cannot be applied directly, because the cross sections depend on the wave length. To use that equation, we have found an equivalent cross section for the total ionizing flux. The ionizing spectrum has been divided into intervals of narrow bandwidth, so that the cross sections can be considered constant inside them. The cross section data corresponding to each interval, σ_k , as well as the solar radiation flux for the same frequencies, Φ_k , have been taken from Kockarts (1973) and a weighted mean, $\bar{\sigma}$, of the cross sections has been taken for each element so that

$$\bar{\sigma} \Phi_T = \sum \sigma_k \Phi_k$$

where Φ_T is the total ionizing solar flux. Then equation 12 can be used taking $\bar{\sigma}$ as cross section and Φ_T as the ionizing flux. The values of the absorption cross sections found for the three elements are:

$$\sigma_O = 6.17 \cdot 10^{-18} \text{ cm}^{-2} ; \quad \sigma_{N_2} = 11.5 \cdot 10^{-18} \text{ cm}^{-2} ; \quad \sigma_{O_2} = 13.39 \cdot 10^{-18} \text{ cm}^{-2}$$

The values for O and N_2 are higher than those of Smith (1968)

$\sigma_O = 5.7 \cdot 10^{-18} \text{ cm}^{-2}$; $\sigma_{N_2} = 7.4 \cdot 10^{-18} \text{ cm}^{-2}$
and lower than those of Yeh et al (1969)

$$\sigma_O = 7.32 \cdot 10^{-18} \text{ cm}^{-2} ; \sigma_{N_2} = 14.1 \cdot 10^{-18} \text{ cm}^{-2}$$

2.4 GRAZING INCIDENCE.

2.4.1 Absorption of radiation.

The optical depth, $\tau = \sigma_0 \int_{z_0}^z n ds$, in eq. 12 gives the ray absorption along the path.

Since we have to obtain the ionization at the sunrise period, grazing incidence of the radiation has to be considered. We shall assume that the ray path is a straight line.

In fig. 2, O represents the centre of the earth, $O-S$ the line joining the centre of the earth with the sun, NTN the surface of the earth and R the earth radius. We shall calculate the absorption of the ray till the point P . To do it, we shall find an expression of the density in a point P' of the ray path, that can be integrated along the ray path.

From fig. 2

$$p = (z + R) \sin \lambda = (z + R) \sin \chi$$

if we call

$$h = \frac{R+z}{H_0} ; h_0 = \frac{R+z_0}{H_0} \quad (13)$$

we obtain

$$z' - z_0 = H_0 \left(h \frac{\sin \lambda}{\sin \lambda} - h \right) = H_0 h \left(\frac{\sin \lambda}{\sin \lambda} - 1 \right) + (z - z_0)$$

To find the density in P' it is enough to substitute $z' - z_0$ in the different terms of the expression of n (cfr. 11). For $T_z^{-\gamma}$ we obtain

$$T_z^{-\gamma} = T_0^{-\gamma} \left[1 - \frac{T_0 - T_0}{T_0} e^{-b H_0 h \left(\frac{\sin \lambda}{\sin \lambda} - 1 \right)} e^{-b(z - z_0)} \right]^{-\gamma}$$

The term to be subtracted in this equation is always smaller than 1 (and much smaller when the altitud is higher) so that only the first terms have to be retained in the development of the power and the equation becomes

$$T^{-\gamma} = T_0^{-\gamma} \left(1 + \gamma \frac{T_0 - T_0}{T_0} e^{-b H_0 h \left(\frac{\sin \lambda}{\sin \lambda} - 1 \right)} e^{-b(z - z_0)} \right)$$

The substitution of $z' - z_0$ in the other terms of eq. 11 is straightforward, and doing

$$\frac{1}{H_0} + b = B ; \quad \frac{1}{H_0} - s = S ; \quad \frac{1}{H_0} + b - s = G$$

$$H_0 h \left(\frac{\sin \lambda}{\sin \lambda} - 1 \right) = \Lambda ; \quad \gamma \frac{T_0 - T_0}{T_0} = T_R$$

it gives

$$n_z = n_0 \cdot T_0 \cdot T_0 \cdot \left[e^{-\frac{z-z_0}{H_0}} e^{-\frac{\Lambda}{H_0}} + T_R e^{-\frac{B(z-z_0)}{H_0}} e^{-\frac{B\Lambda}{H_0}} + k(z-z_0) e^{-\frac{S(z-z_0)}{H_0}} e^{-\frac{S\Lambda}{H_0}} + T_R k(z-z_0) e^{-\frac{G(z-z_0)}{H_0}} e^{-\frac{G\Lambda}{H_0}} + k e^{-\frac{S(z-z_0)}{H_0}} e^{-\frac{S\Lambda}{H_0}} + T_R k e^{-\frac{G(z-z_0)}{H_0}} e^{-\frac{G\Lambda}{H_0}} \right] \quad (14)$$

The ds that appears in τ is (cf. fig. 2)

$$ds = \frac{(R+z) d\lambda}{\sin \lambda} = \frac{(R+z) \sin \chi}{\sin^2 \lambda} d\lambda$$

or, according to (13)

$$ds = H_0 h \sin \chi \operatorname{cosec}^2 \lambda d\lambda$$

with the limits of the integral of τ $0 \leq \lambda \leq \chi$

To calculate the integral we assume that H_0 is independent of λ and its value is equal to the one that corresponds to $\lambda = \chi$. Since $R \gg z$ in the region where most of the ionization is accumulated, the sum $R + z$ is taken as constant and equal to 6.700 Km. With these conditions, we find the following expression for the optical depth

$$\tau = K_0 K_1 e^{-\frac{z-z_0}{H_0}} + K_2 e^{-\frac{B(z-z_0)}{H_0}} + K_3 (z-z_0) e^{-\frac{S(z-z_0)}{H_0}} + K_4 (z-z_0) e^{-\frac{G(z-z_0)}{H_0}} + K_5 e^{-\frac{S(z-z_0)}{H_0}} + K_6 e^{-\frac{G(z-z_0)}{H_0}} \quad (15)$$

where

$$K_0 = H_0 h \sin \chi \sigma_a n_0 T_0^{-1} T_0^{-1}$$

$$K_1 = \int_0^{\chi} e^{-\frac{\Lambda}{H_0}} \operatorname{cosec}^2 \lambda \, d\lambda$$

$$K_2 = T_R \int_0^{\chi} e^{-B\Lambda} \operatorname{cosec}^2 \lambda \, d\lambda$$

$$K_3 = k \int_0^{\chi} e^{-S\Lambda} \operatorname{cosec}^2 \lambda \, d\lambda$$

$$K_4 = T_R k \int_0^{\chi} e^{-G\Lambda} \operatorname{cosec}^2 \lambda \, d\lambda$$

$$K_5 = k \int_0^{\chi} \Lambda e^{-S\Lambda} \operatorname{cosec}^2 \lambda \, d\lambda$$

$$K_6 = T_R k \int_0^{\chi} \Lambda e^{-G\Lambda} \operatorname{cosec}^2 \lambda \, d\lambda$$

All these integrals are independent of z and can be obtained by a numerical integration. The integrals K_1 to K_4 have the same form and only differ in the constant coefficient that multiply the factor

$$\Lambda \equiv H_0 h \left(\frac{\sin \chi}{\sin \lambda} - 1 \right)$$

The products $K_0 K_1$ ($i=1,4$) have the form of the Chapman function (cfr. Chapman 1931). In fact, $K_0 K_1$ is the Chapman function for a scale height H_0 . This means that integrals K_2 to K_6 give the modification of present model as compare with a Chapman layer.

2.4.2 Production rate.

The expression for the production rate is easily obtained by substituting the optical depth of eq. 15, into eq. 12. For the production rate of the j component it gives

$$q_j = \Phi_{\infty} \sigma_{ij} n_j e^{-\sum_i K_i e^{-\frac{z-z_0}{H_{\infty}}}} \left[K_{1i} + K_{2i} e^{-b(z-z_0)} + (K_{3i}(z-z_0) + K_{5i} e^{s(z-z_0)} + (K_{4i}(z-z_0) + K_{6i} e^{-(b-s_i)(z-z_0)}]) \right] \quad (17)$$

where n_j is a function of height and is given by (11). To compare the ionization production rate of the three components, O, N₂ and O₂, the distribution curves of q_j with height have been obtained for several exospheric temperatures assuming an ionization efficiency equal to 1. The results are shown in fig. 3. For the solar flux, the value $O = 5.24 \cdot 10^{10} \text{ cm}^{-2} \text{ s}^{-1}$ has been taken, that corresponds to the sum of the fluxes for the different wave lengths between 910 and 80 Å given by Kokarts (1973).

As can be seen, the contribution of the O₂ production rate to the total ionization is very small, so that it can be neglected for the calculation of the total electron production.

For such a calculation we have assumed that the ionization efficiency of the atomic oxygen is equal to unity and that of N₂ equal to zero, that is

$$\sigma_{iO} = \sigma_{aO} \quad ; \quad \sigma_{iN_2} = 0$$

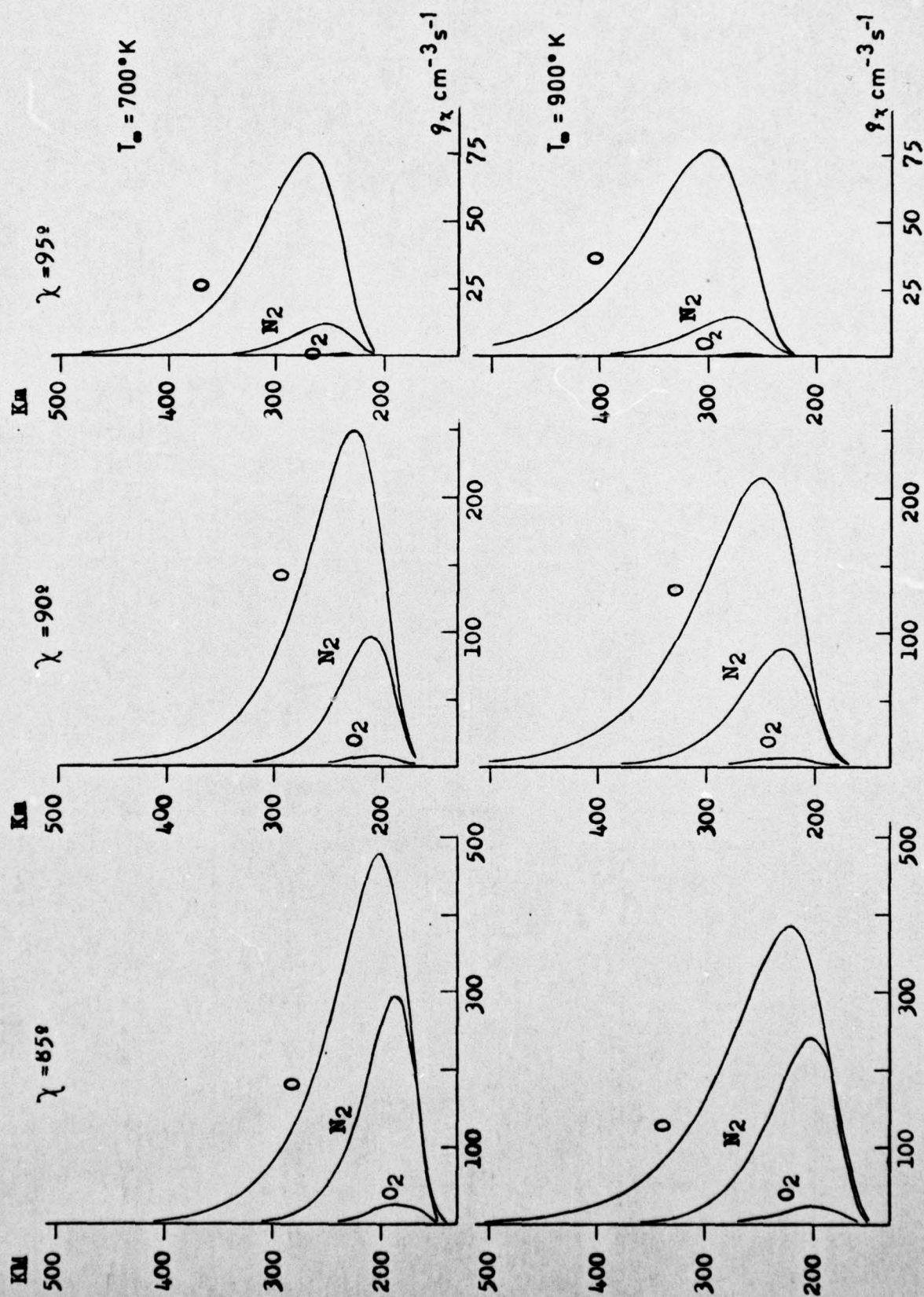


fig. 3. - Ionization rate profiles for different sun positions and exospheric temperatures

The first hypothesis agrees with the experimental results (cf. Whitten and Poppoff (1971)). The second one is an approximation based, first of all, on the fact that only small number of N_2^+ ions have been found in the thermosphere (cfr. for instance Narcisi (1975)). This indicates that N_2^+ ions disappear so quickly that its contribution to the total ionization is negligible. On the other hand the reactions for the N_2^+ ions disappearance, do not produce other long life ions that could contribute to the ionization.

With these assumptions, the production rate of electrons is practically the same as the ionization production rate of the atomic oxygen. Its expression is the same of eq. 17 with the j component being the atomic oxygen and the sum of the exponential being extended to O and N_2 .

In order to compare with the experimental data we need the total electron content. The production rate, q , has then, to be integrated, to obtain the integrated production rate Q . This integration yields

$$Q_x = \sigma_{i_{ox}} n_{ox} \left[\frac{I_0}{I_m} \right] \Phi_{ox} \int_{z_0}^{z_m} \left[1 - \frac{I_m - I_0}{I_m} e^{-b(z-z_0)} \right] e^{-\frac{z-z_0}{H_{ox}}} \left[1 + k_{ox}(z-z_0) e^{s_{ox}(z-z_0)} \right] \times$$

$$\times e^{-\sum_i K_i} e^{-\frac{z-z_0}{H_{ox}}} \left[K_1 + K_2 e^{-b(z-z_0)} + (K_3(z-z_0) + K_5) e^{s(z-z_0)} + (K_4(z-z_0) + K_6) e^{-(b-s_1)(z-z_0)} \right] dz \quad (18)$$

where we put Q_{χ} to indicate the dependence of the zenithal angle of the sun through K_{χ} and where all dependence of z has been explicitated.

In fig. 4, the curves $Q(\chi)$ between $85^{\circ} \leq \chi \leq 100^{\circ}$ are shown for two exospheric temperatures. These curves are obtained from eq 13 considering the upper limit of integration $z_{\infty} = 500\text{Km}$ since, as it can be seen in the curves of fig. 3, the production rate above this region is almost zero.

The two curves of fig. 4 are almost parallel. This means that both curves can be reduced to a common one if they are normalized by a convenient factor. Smith (1968), with a model of an isothermal neutral atmosphere, with two components whose production profiles are derived from the Chapman theory, found that, normalizing the Q curves with respect to its value for $\chi = 90^{\circ}$, the shape of the curves Q / Q_{90} is almost independent of the concentration relation of both components. We have applied a similar normalization to the present model and have found that the curves Q / Q_{90} are almost independent of the exospheric temperature. This can be seen in fig. 5 where the curves corresponding to exospheric temperatures $T_{\infty} = 700^{\circ}\text{K}$ and $T_{\infty} = 1000^{\circ}\text{K}$ are shown. This property of the quasi-independence of Q / Q_{90} from the exospheric temperature, shall be utilized later on to deduce the value of Q_{90} .

2.5 IONIZATION LOSS RATE.

As it is known most of the O^+ ions disappear through the process of reactions



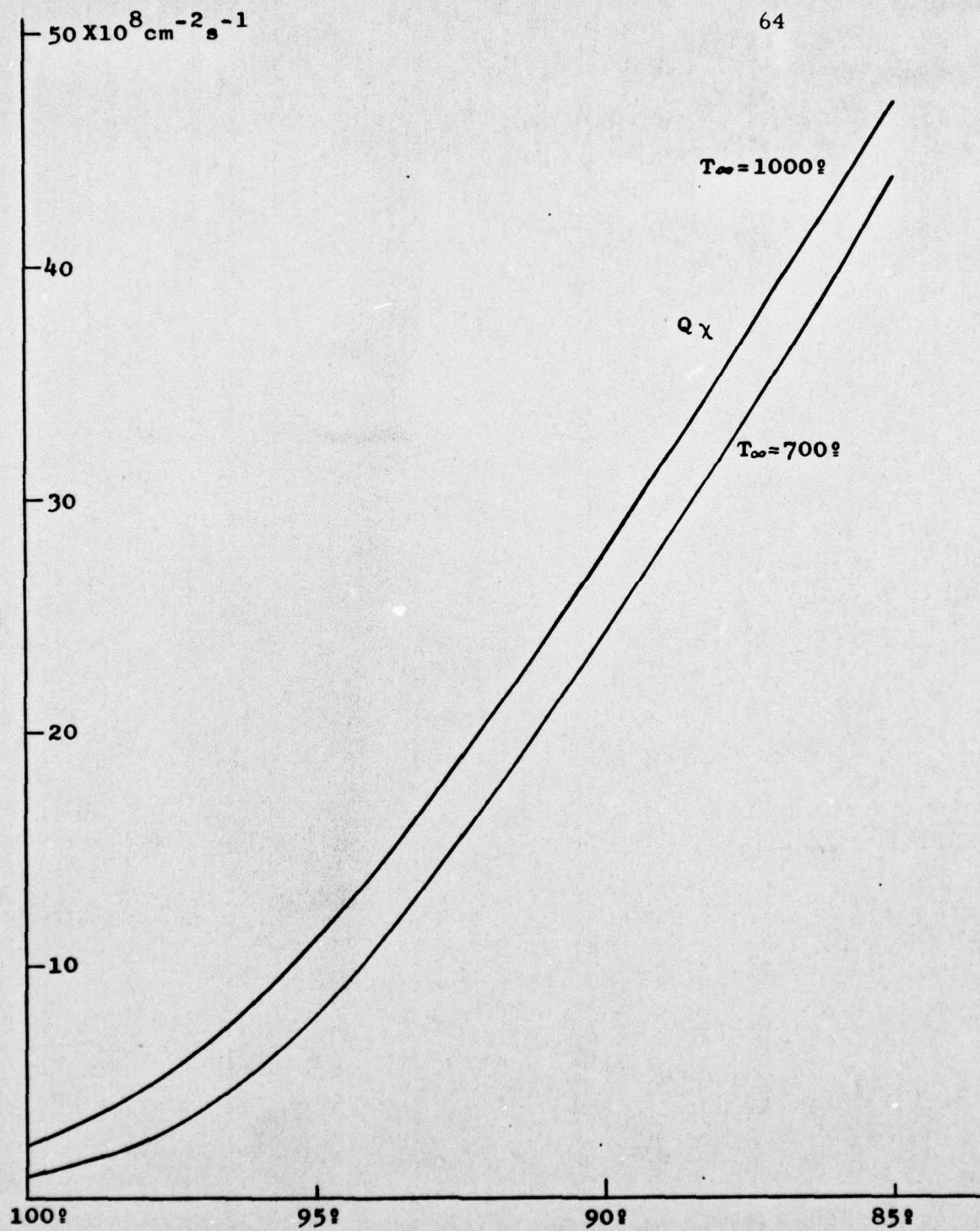


fig. 4. - Integrated ionization production rate

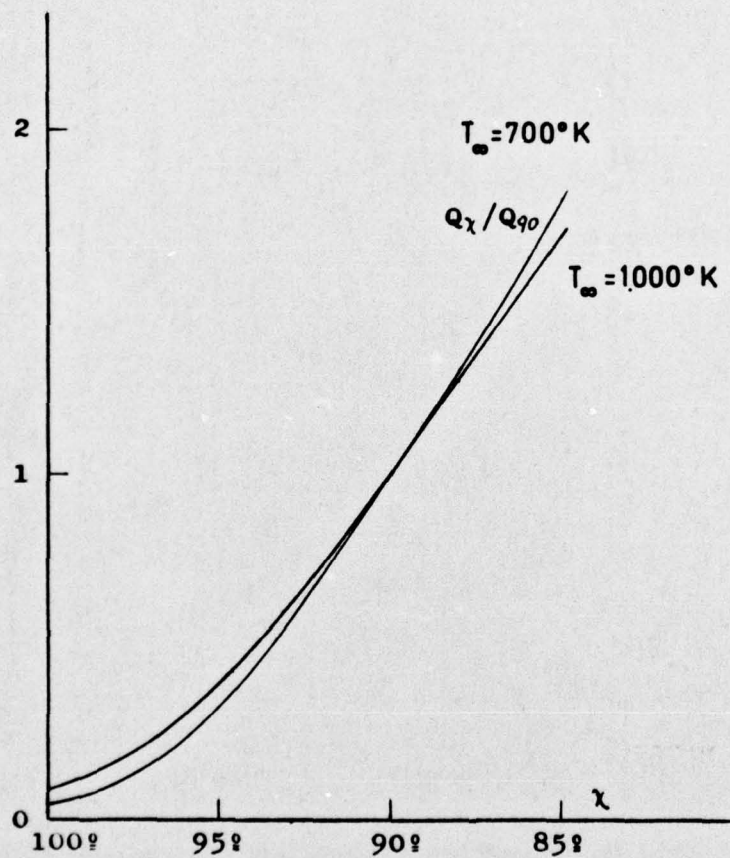


fig. 5. - Integrated ionization production rate, normalized with respect to Q_{90} , as a function of the zenithal angle of the sun

The ion O^+ is dominant in the region between about 200 and 500Km, where most of the ionization is present. It seems then reasonably to conclude that reaction 19-b is much more rapid than reaction 19-a, so that, as a first approximation, we can assume that the ionization loss rate is equal to the rate of occurrence of reaction 19-a.

According to this, the ionization loss rate is

$$I = C_a n [O^+] n [N_2] \quad (20)$$

where C_a is the loss coefficient of reaction 19-a and $n [X]$ indicates concentration of the X element.

As we have said, eq. 20 is only an approximation but, since during, the sunrise period the ionization loss is very small, an error in its determination cannot be very important.

Because of the neutrality of the ionosphere, we can also approximate $n [O^+] = n [e^-]$ and eq. 20 becomes

$$I = \beta n [e^-] \quad (21)$$

where

$$\beta = C_a n [N_2]$$

For the variation of β with height, we have used the simple model

$$\beta = \beta_0 e^{-\frac{Z-Z_0}{H_{N_2}}} \quad (22)$$

where H_{N_2} is the scale height of N_2 corresponding to the temperature T_∞ . The use of the variation of the N_2 density given by the more sophisticated model of this report to calculate β , would

complicate the calculation without appreciably increasing its accuracy.

The value of the coefficient β_e , that appear in eq. 22, has been obtained from the value of β at a height of 300Km, given by Smith (1968), $\beta_{300} = 1.4 \cdot 10^{-5} s^{-1}$.

2.6 TOTAL ELECTRON CONTENT VARIATION.

With the simplification related to the movement term, and taking into account eq. 21 and 22, the continuity equation (1) becomes

$$\frac{\partial N(z,t)}{\partial t} = q(z,t) - \beta_e e^{-\frac{z-z_0}{H_{eN_2}}} N(z,t) \quad (23)$$

where the dependence from the z and t variable has been shown. The expression for $q(z,t)$ is given in eq. 17 and depends on t through the zenithal angle of the sun.

To compare with the experimental total electron content data, we have to solve the continuity equation (23) and calculate afterwards, the integral for the different values of t at which data have been recorded.

To solve eq. 23, we fix as the initial moment, t_0 , the time when $\chi = 100^\circ$, since the photoionization is practically zero for greater values of χ and the experimental total electron content usually do not increase before this time.

Using a method similar to the one utilized by Smith (1968) the total electron content is divided into two parts, the nighttime ionization, or ionization present at the initial moment $t = t_0$, and the ionization produced from this moment onwards. Both parts can be

treated separately because of the linearity of eq. 23.

The second part of the electron content can be found by numerically solving eq. 23 with the initial condition $N(z, t_0) = 0$, and integrating afterwards $N(z, t)$ with respect to z . For the nighttime ionization, we assume that its evolution during the time between $100^\circ \geq \chi \geq 87^\circ$ (at which the calculations are extended) is the same as during the hour before the initial moment $t = t_0$ (or $\chi = 100^\circ$). The limit of $\chi = 87^\circ$ is imposed because the validity of the approximation (21) is questionable after that time. In the fig. 6 an example of the variation of TEC from an hour before $\chi = 100^\circ$ is shown. As it can be seen, the variation till $\chi = 100^\circ$ can be fitted by a straight line of negative slope. If no new ionization were produced, the electron content, N_p , at any time, t , of the interval $100^\circ \geq \chi \geq 87^\circ$ should be

$$N_p = N_{T_0} - b(t - t_0)$$

where N_{T_0} is the electron content at the initial moment, t_0 , and $-b$ is the slope of the fitted line. N_p is, then, the amount of ionization present at time t , due to the nighttime ionization; adding it to the ionization produced from the initial moment, t_0 , till time t , we obtain the total electron content at this time.

The slope $-b$ is obtained by fitting a straight line to the experimental TEC data. N_{T_0} can be obtained directly from the records or by the procedure that we give below.

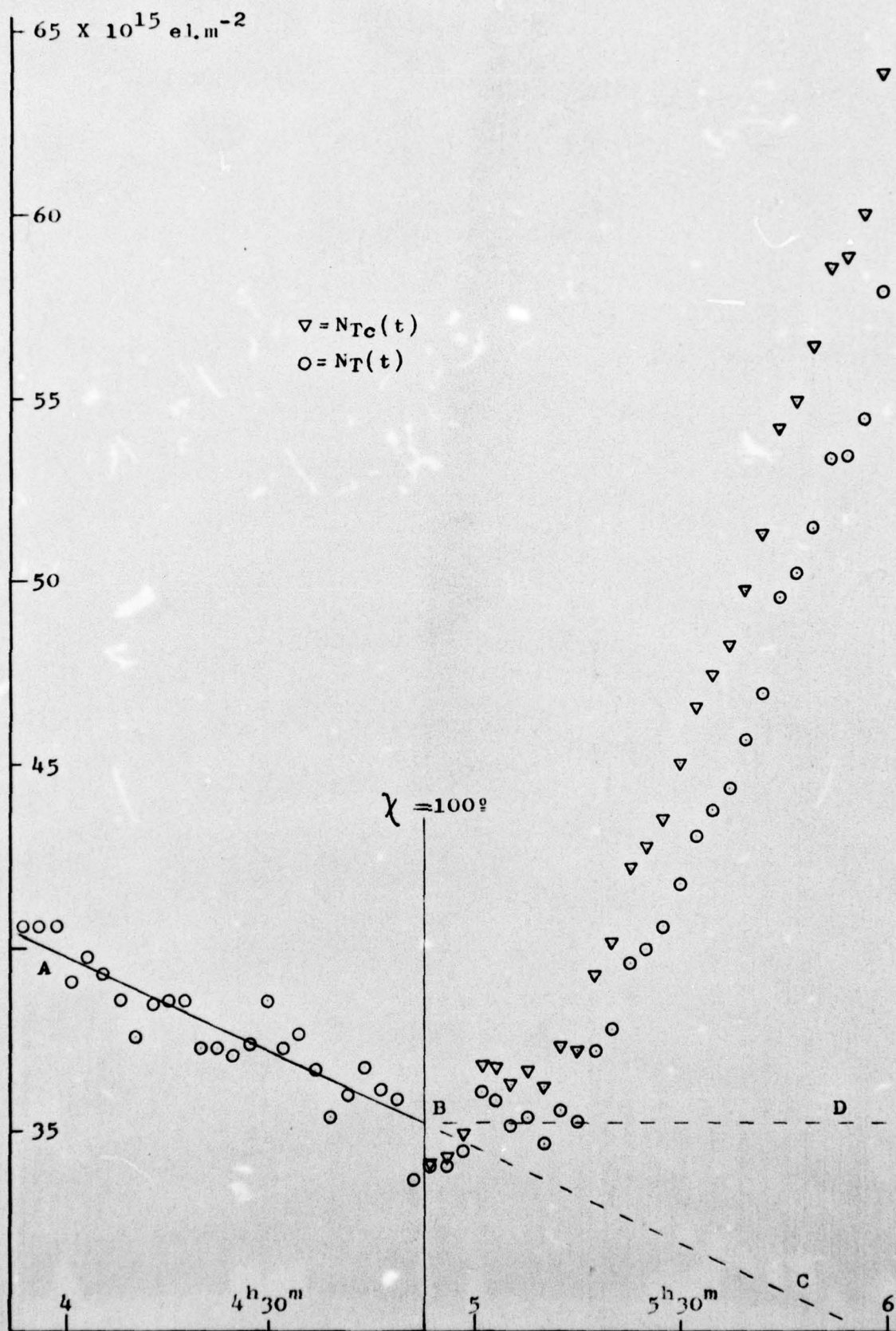


fig. 6. - Total electron content (N_T) and its values corrected for the effect of the nighttime ionization

2.7 INTEGRATED PRODUCTION RATE FOR $\chi = 90^\circ$

If we substitute $q(z,t)$ by $q(z,t)/Q_{90}$, equation 23 becomes

$$\frac{\partial N_R(z,t)}{\partial t} = \frac{q(z,t)}{Q_{90}} - \beta e^{-\frac{z-z_0}{H}} N_2 N_R(z,t) \quad (24)$$

with

$$N_R(z,t) = \frac{N(z,t)}{Q_{90}}$$

Solving this equation with the initial condition $N_R(z, t_0) = 0$, instead of $N_T(t)$ we obtain

$$N_{IR} = N_{II}(t)/Q_{90}$$

where N_{II} indicates the total electron content produced by photoionization from the initial moment t_0 till time t . Then, the total electron content is:

$$N_I(t) = N_{I_0} - b(t-t_0) + Q_{90} N_{IR}(t)$$

and putting

$$N_{IC}(t) = N_I(t) + b(t-t_0) \quad (25)$$

results

$$N_{IC}(t) = N_{I_0} + Q_{90} N_{IR}(t) \quad (26)$$

that gives Q_{90} as the slope of the linear correlation between the values of N_{IC} and N_{IR} .

The values of N_{IC} are obtained by correcting the experimental data of TEC for the nocturnal ionization, as it is shown in fig. 6. The N_{IR} are the theoretical values of TEC normalized with respect to Q_{90} , obtained by solving eq. 24.

The correlation of these series of values gives also

the TEC at the initial moment N_{T0} .

The use of eq. 24 instead of eq. 23 has the advantage that the values of N_{TR} depend on the Q/Q_{90} relation that, as we have indicated, is almost independent of the exospheric temperature, T_{∞} , from which the parameters of the equation are derived. On the other hand, in eq. 24, q values are substituted by q/Q_{90} and, while q directly depends on the solar flux, q/Q_{90} is independent of this parameter. Also the dependence of q on the product of the oxygen cross section and the oxygen density at the z_0 level ($\sigma_{ox} \cdot n_{ox}$) is stronger than dependence of q/Q_{90} on the same product. Therefore, any error in the determination of these parameters has much less influence in the value of Q_{90} if it is calculated by eq. 24 than if it is done by eq. 23.

3. RESULTS.

3.1 VALUES AT OBSERVATORIO DEL EBRO.

The method just described has been applied to the TEC data obtained in the Observatorio del Ebro during the period August 1973-July 1974, to deduce daily values of Q_{90} . As we have seen, this requires the determination of daily values of N_{TR} during the interval $100^{\circ} > \chi > 87^{\circ}$ which, in turn, requires the determination of the exospheric temperature for the same interval. As we have already said, T_{∞} has been calculated by the method given by Jacchia (1971). In this method, it is assumed that there is no semiannual variation of the exospheric temperature. On the contrary, in his model of 1970, Jacchia incorporates a semiannual variation of T_{∞} to account for the semiannual variation of density deduced

ced from the satellite drag data. The semiannual variation of T_{∞} , calculated according to the Jacchia (1970) model, gives a maximum oscillation of $\pm 40^{\circ}$ for the period August 1973- July 1974. The incorporation of this variation to T_{∞} would not change substantially the results obtained in this report, since, as has been shown, the influence of T_{∞} on the Q_{90} calculation is very small in the method used. For the same reason, we have neglected the small variation of T_{∞} during the interval $100^{\circ} > \chi > 87^{\circ}$ and have taken it as constant equal to its value at $\chi = 90^{\circ}$.

In fig.7 some examples of the representation of the N_{Tc} and N_{TR} values are given. The slope of these lines is the value of Q_{90} . In some cases it seems that N_{TR} only starts increasing several minutes after $\chi = 100^{\circ}$. In these cases two linear correlations have been obtained, the first one including all the points while in the second one the points before the first four increasing values, have been eliminated. In general both correlations are very similar and only in few cases where the first one gives an absurd result ($Q_{90} < 0$) the difference has been significant. Therefore, the second correlation has been taken as the valid one in determining Q_{90} .

The values of Q_{90} obtained for the whole period August 1973-July 1974 are shown in fig. 8 where also the running mean of 27 days of these values is given. The smoothing of the Q_{90} values has been used to eliminate the possible influence of the rotation period of the sun. Although there is a certain dispersal of the points, some sort of semiannual variation is clearly appreciated that is better seen in the running mean curve. In this curve, one maximum occurs about the 20 of October and another one at the end of February or beginning of March. This second one seems to be a little lower. The

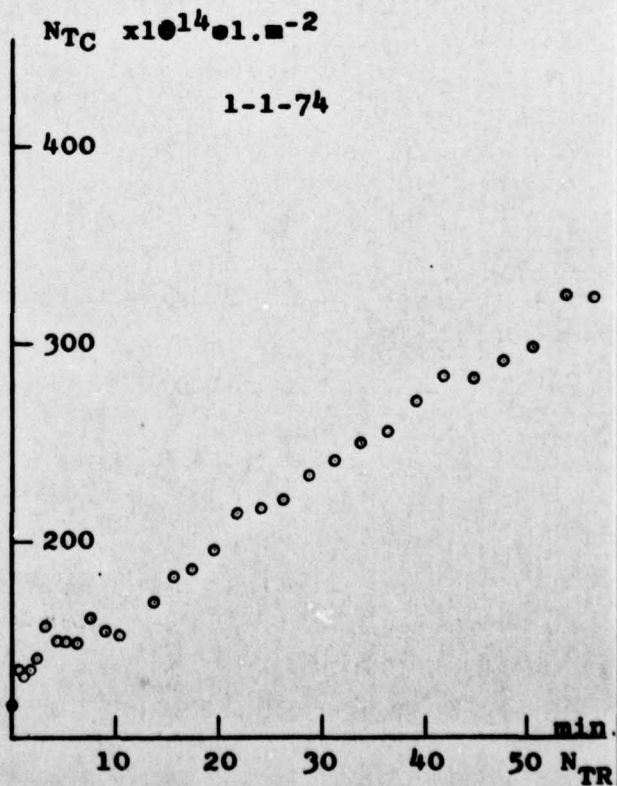
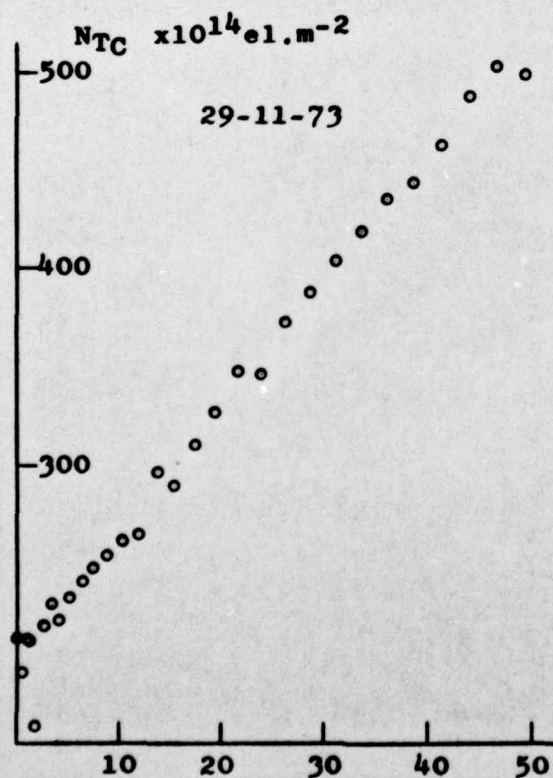
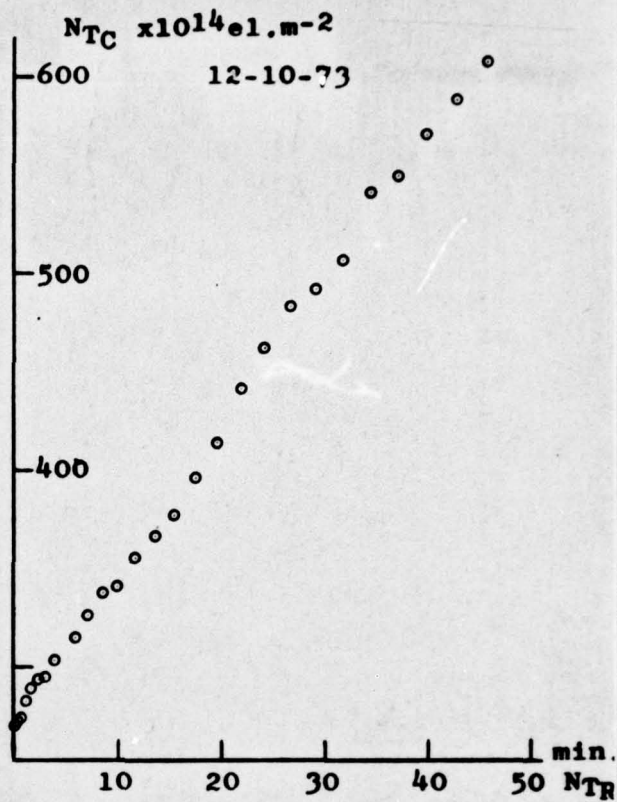
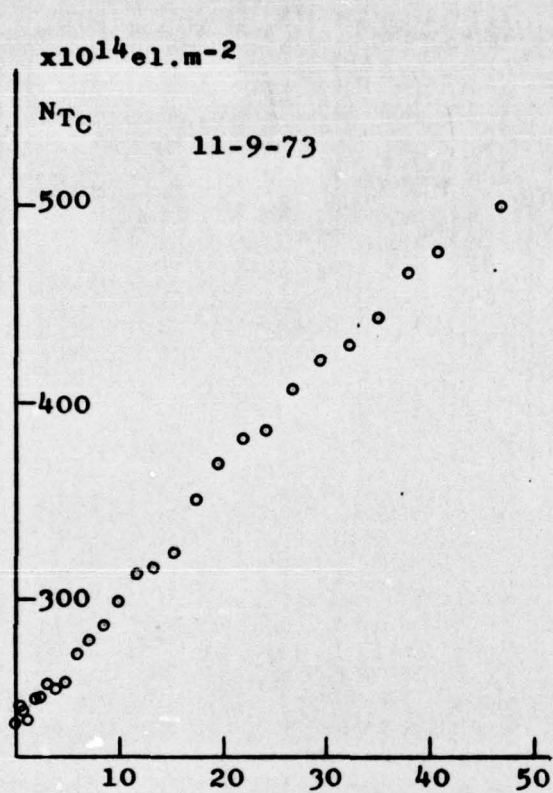


fig. 7. - Representation of the N_{TC} - N_{TR} values

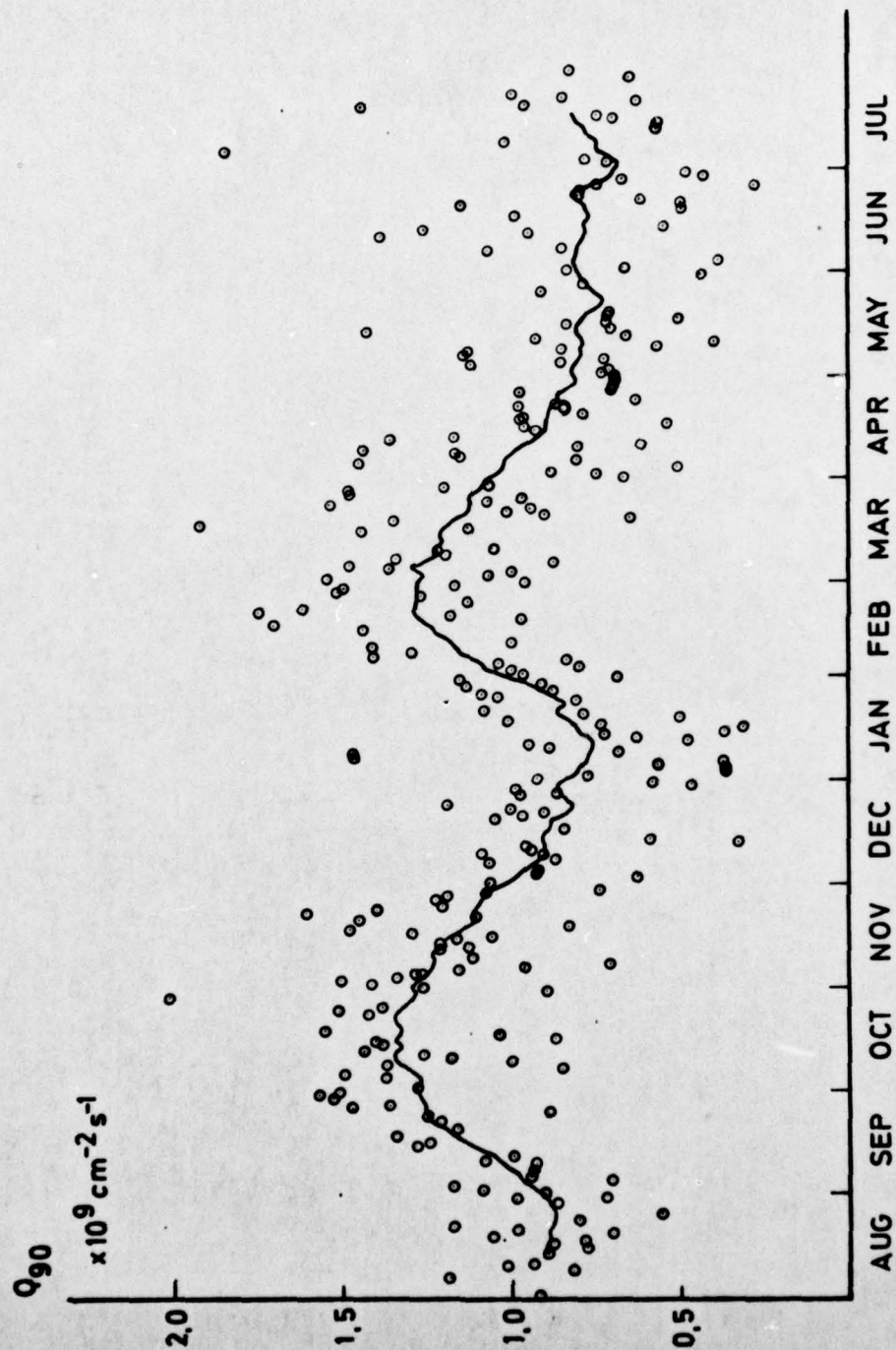


fig. 8. - Daily Q_{90} values and its 27 days running mean

minimum at the end of June or the beginning of July is also lower than the one at about 12 of January. The minimum of summer is less sharp than the one in winter perhaps because of a bigger dispersal of the values since the month of March. The dispersal may be caused by reflections of the incoming wave in an obstacle placed towards the west of the receiving antenna. The satellite had a shift towards the west and we have to move the antenna in that direction, so that the values of the last months can be a little affected by reflections in the mentioned obstacle.

If the difference between the values of summer and winter is significant, it could indicate the existence of an annual variation, besides the semiannual one, although smaller than that.

An harmonic analysis of all the points gives a mean value of $Q_{90} = 1.010^9 \text{ cm}^2 \text{ s}^{-1}$ a first harmonic of amplitude 15% of the mean value and a second harmonic of 20% amplitude. If the two harmonics are expressed in the form $R \cos(k\omega t + \varphi_k)$, the phases are $\varphi_1 = 29.6^\circ$ and $\varphi_2 = 185.3^\circ$ beginning on January 1st, that corresponds to an annual variation with maximum on December 1st and minimum on July 1st, and a semiannual variation with maxima on 28 September and 29-30 March, and minima on 28 December and 29 June.

In fig. 9 the running mean and the curve resulting of the two harmonics are represented for comparison.

3.2 COMPARISON WITH OTHER AUTHORS.

3.2.1 Mean value

Smith (1968) analyzes the Faraday rotation data obtained in Hawaii (21°N) with a model of isothermal neutral atmosphere of two components (N_2 and O), based on data

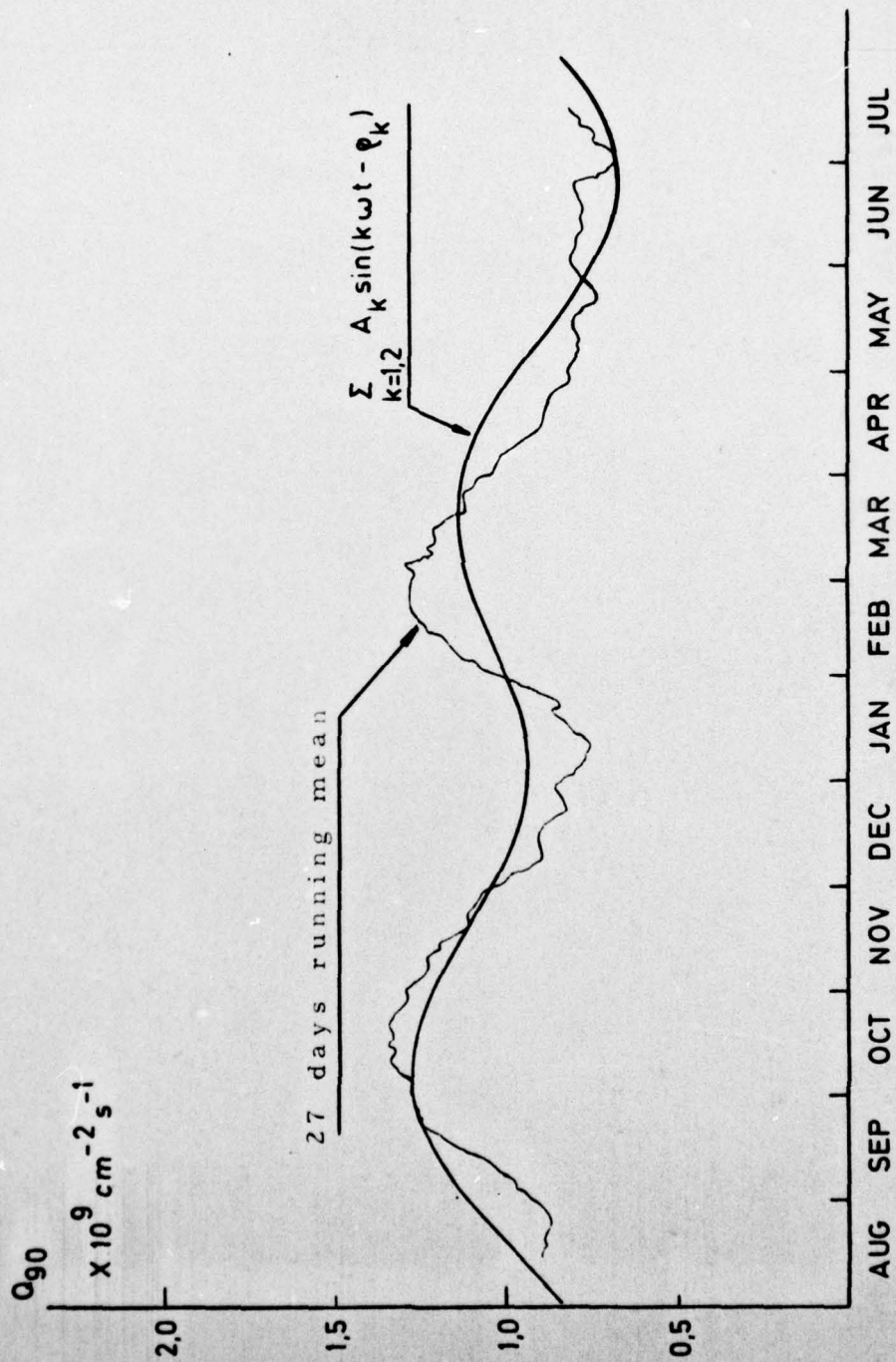


fig. 9. - Running mean and harmonic analysis of Q_{90}

of the Cira (1965) model, and whose production profile he deduces from the Chapman theory. He finds a mean value of $Q_{90} = 1.7 \cdot 10^9 \text{ cm}^2 \text{ s}^{-1}$ for the period Sept. 1964-August 1966 that includes a minimum of solar cycle. With the same method, Spurling (1972) finds daily values of Q_{90} in Bribie Island (27°S 153°E) for the period Oct 1969-Sept. 1970 of high solar activity. The days running mean of these values remains between 2.10 and $3.3 \cdot 10^9 \text{ cm}^2 \text{ s}^{-1}$. The differences of these values with the value $1.0 \cdot 10^9 \text{ cm}^2 \text{ s}^{-1}$ obtained at Ebro, can be due to a latitudinal variation of Q_{90} that diminishes with increasing latitudes and to a variation with the solar cycle.

Tyagi and Mitra (1970), with data of the BE-C satellite, find for Delhi (28.6°N) summer Q_{90} values from $0.93 \cdot 10^9$ for very low solar activity to $2.8 \cdot 10^9 \text{ cm}^2 \text{ s}^{-1}$ for high solar activity. These authors assume an isothermal atmosphere of only one component and do not consider the night time ionization, so that the values of Q_{90} should probably be a little higher. Assuming a 30% loss due to nighttime ionization, that is about the one calculated in this report, the minimum value of Q_{90} should be $1.3 \cdot 10^9 \text{ cm}^2 \text{ s}^{-1}$ slightly higher than the value of obtained at Ebro; these results are in agreement with the latitudinal variation.

Other authors, employing in general, an isothermal neutral atmosphere of only one component, find the integrated production rate for an overhead sun (Q_0). In order to compare their results with the ones at Ebro, we calculated the value of Q_0 that corresponds to our mean value of Q_{90} for an exospheric temperature $T_{\infty} = 770^\circ\text{K}$, that is the mean temperature during the period covered by our data. The obtained value is $Q_0 = 0.97 \cdot 10^{10} \text{ cm}^2 \text{ s}^{-1}$, slightly higher than the one

found by Titheridge (1966) $0.9 \cdot 10^{10} \text{ cm}^{-2} \text{ s}^{-1}$ and lower than the values of Garriot and Smith (1965) $1.4 \cdot 10^{10} \text{ cm}^{-2} \text{ s}^{-1}$, Taylor (1965) $1.0 \cdot 10^{10} \text{ cm}^{-2} \text{ s}^{-1}$ for thirteen summer days and $2.4 \cdot 10^{10} \text{ cm}^{-2} \text{ s}^{-1}$ for eight winter days, Majid and Bhuriwala (1976) $1.7 \cdot 10^{10}$, $1.0 \cdot 10^{10}$ and $1.45 \cdot 10^{10} \text{ cm}^{-2} \text{ s}^{-1}$ respectively for winter, summer and equinoxes during a minimum of solar activity and $2.7 \cdot 10^{10}$, $1.87 \cdot 10^{10}$ and $2.4 \cdot 10^{10} \text{ cm}^{-2} \text{ s}^{-1}$ for the same seasons and high solar activity, and Koster (1976) between about $2.6 \cdot 10^{10} \text{ cm}^{-2} \text{ s}^{-1}$ for low solar activity, and $6 \cdot 10^{10} \text{ cm}^{-2} \text{ s}^{-1}$ for a maximum of the solar cycle. The lowest value of Q_0 mentioned above, is that of Titheridge (1966), and corresponds to a station of the southern hemisphere, Auckland (subion. 34°S) during a period of low solar activity. All other values belong to the northern hemisphere and, except for the data of Taylor (1965), correspond to latitudes well below that of Ebro: Koster (1976) at Legon (5°6°N), Garriot and Smith (1965) at Hawaii (subion. 20°N) and Majid and Bhuriwala (1976) at Karachi (25°N). The values given by Taylor (1966), although correspond to a latitude of 48°N greater than the one at Ebro, they were obtained during a period of high solar activity. This explains that his values are bigger than the Ebro's, of lower latitude, but obtained in a period of low solar activity.

Rao (1967) obtains the production rate, q_0 , for an overhead sun, in the maximum of the F layer, from TEC data derived from the signal of the BE-C satellite. The satellite signals were recorded in Urbana (40°N) during the period August-September 1965 of low solar activity. He finds $q_0 = 0.638 \cdot 10^9 \text{ m}^{-3} \text{ s}^{-1}$. Assuming a Chapman layer with only one component, the production rate in the maximum of the layer, q_0 , can be related with the integrated production rate for an overhead

sun, Q_0 , and the scale height, H , through the equation $Q_0 = e H q_0$, where $e = 2.718$. Assuming a value of scale height $H = 50\text{Km}$, corresponding to the oxygen, we obtain $Q_0 = 0.87 \cdot 10^{10} \text{ cm}^{-2} \text{ s}^{-1}$, very near to the value of Ebro (of similar latitude). The similarity is higher if we consider that in the Q_0 calculation of Urbana the nighttime ionization has not been taken into account.

3.2.2 Annual and semiannual variation.

Among all the authors just mentioned, only Smith (1968) and Spurling (1972) employ a model of two components to deduce the ionization production rate, and neither of them find significant periodic variations of Q . With respect to the rest of the authors, we have already mentioned that Taylor (1965) finds higher values in winter than in summer, but the number of days analyzed is so small that it is difficult to draw any final conclusion. Also Majid and Bhuriwala (1976) find higher values in winter than in summer, independently of the solar activity. They find that at any level of solar activity the Q values in equinoxes are lower than in winter and higher than in summer, what indicates an annual variation with maximum in winter and minimum in summer. At the same result arrive Risbeth and Setty (1961) considering the electronic density variation during sunrise at fix heights, obtained with a ionosonde of vertical incidence.

Results more similar to ours are obtained by Titheridge (1974). This author finds, for a period of increasing solar activity, a semiannual variation of Q_0 with maxima in March-April and September-October, superimposed to an annual variation with maximum in January-February, for the stations of Hawaii and Stanford (sub

ion 34°N). For the southern station of Auckland, he finds only the semiannual variation. Although this author finds values of Q_0 and not of Q_{90} , the variation of both parameters should be similar.

Koster (1976) performs an harmonic analysis of the data given by Titheridge and those obtained by himself in the equatorial station of Legon. He finds a first harmonic (annual variation) of amplitude between 12 and 22% of the mean value in the northern stations and only of 3% in Auckland. The amplitude of 15% found for Ebro, agrees with the values of the northern stations. For the second harmonic (semiannual variation) he finds values between 8 and 10% for the four stations, about half of the 20% amplitude of Ebro. With respect to the phases he finds for the first harmonic 233° for Auckland and between -14° and 19° for the others. The Ebro result, 29.6° , is still comparable with the northern stations. The phases of the second harmonic for the northern stations are very similar, 161 and 162° , reaching 172° in Auckland, that is the nearest value to the 185° of Ebro. Also Auckland is the only station, among the four analyzed by Koster, whose semiannual variation is bigger than the annual one, the same that happens in Ebro.

Alberca and Galdón (1974), with a model of only one component, obtained daily values of Q_0 , by fitting a second degree polynomial to the T.E.C. data at sunrise at the Observatorio del Ebro. The variation of Q_0 for the first six months of 1974 was different from the one found in the present report. A more recent study of the method seems to indicate that the second degree polynomial approximation, did not express the variation of the TEC at sunrise with enough accuracy to obtain the value of Q_0 through the procedure there indicated. In fact, the coefficient of the second degree

term that was used in the determination of Q_0 , was very sensitive to the interval in which the fitting was performed. In some cases the inclusion (or exclusion) of only one value of TEC was enough to produce a change of the coefficient. On the other hand, the first value taken for the fitting, was the nearest to the moment at which $\chi = 100^\circ$. But many times, at this point, the TEC is still decreasing, so that the coefficient of the first degree term of the polynomial is negative. As a consequence the coefficient of the second degree term has to be bigger to be able to fit the increasing part of the curve. This negative coefficient has a seasonal variation and its effect is different on the different seasons.

As an indication of this seasonal variation, the slopes of the straight lines fitted to the values of TEC during the hour before to $\chi=100^\circ$, are given in fig. 10. As can be seen, in April and May, the slope is more negative than in winter, a result that can justify the form of the curve found by the mentioned method. If, the values of TEC are corrected for the nighttime ionization (through a similar procedure to the one adopted in this report) before the fitting of the polynomial then, different values of Q_0 are obtained. The results obtained by this method, are a little more similar to those of the present report. This seems to indicate that, although the electron loss at sunrise is very small, it affects the shape of the electron content variation during this period, so that not always can be accurately represented by a second degree polynomial.

Another cause for the discrepancy of the results found by both methods, may be the already mentioned when explain the dispersion of the values of the last

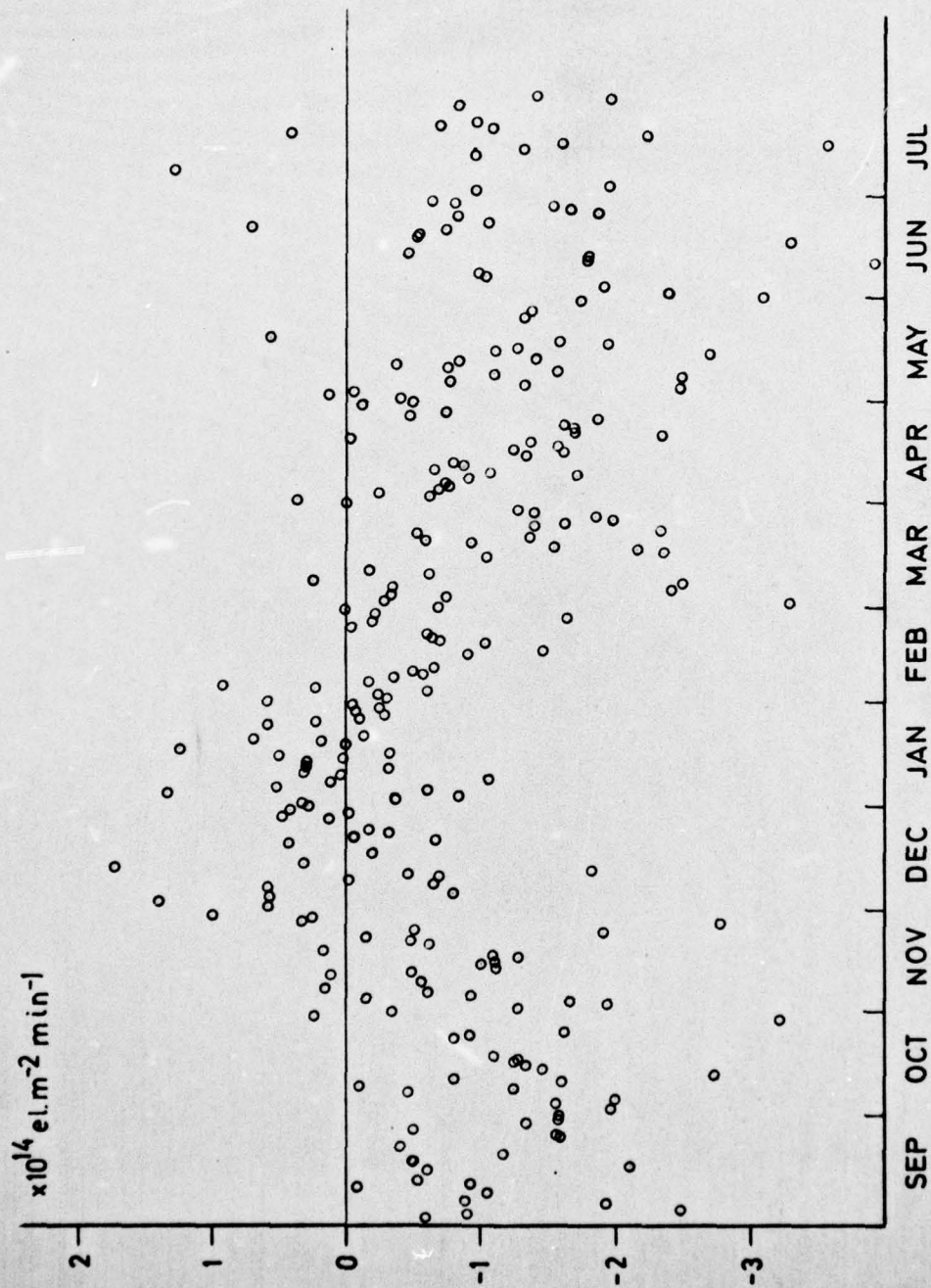


fig. 10. - Daily values of the slope of the total electron content during the hour before to $\chi = 100^\circ$

analyzed months. That is, the distortion of the electron content curve, due to reflections of the incoming signal by an obstacle not far from the receiving antenna, and that was more effective during the last months. The curves of fig. 11 seem to confirm this explanation. They are the running mean curves of Q_0 and Q_{90} for the period August-December 1973, obtained, respectively, by the methods described in the 1974 report and in the present one. As it can be seen, the variation of both curves is very similar in this period, in which the mentioned distortion was not present.

3.3 DISCUSSION.

In fig. 12 besides the Q_{90} running mean curve, we show the values of the exospheric temperature, T_{∞} , used in this report, with its running mean of 27 days and the mean daily solar flux in 10.7 cm, $F_{10.7}$ as well as its running mean for three solar rotations, $\bar{F}_{10.7}$.

As can be seen, besides the variation due to the solar rotation, the daily solar flux has another small variation during this period, with the winter values slightly lower than those of summer. This last small variation is better appreciated in the running mean curve.

The variation of the exospheric temperature and its running mean is, as expected, similar to the variation of the solar flux.

About the Q_{90} curve, perhaps the difference between the two maxima could be related to the difference of solar activity of the two periods. To the same cause could be attributed the difference between the values of August and January, although such differen-

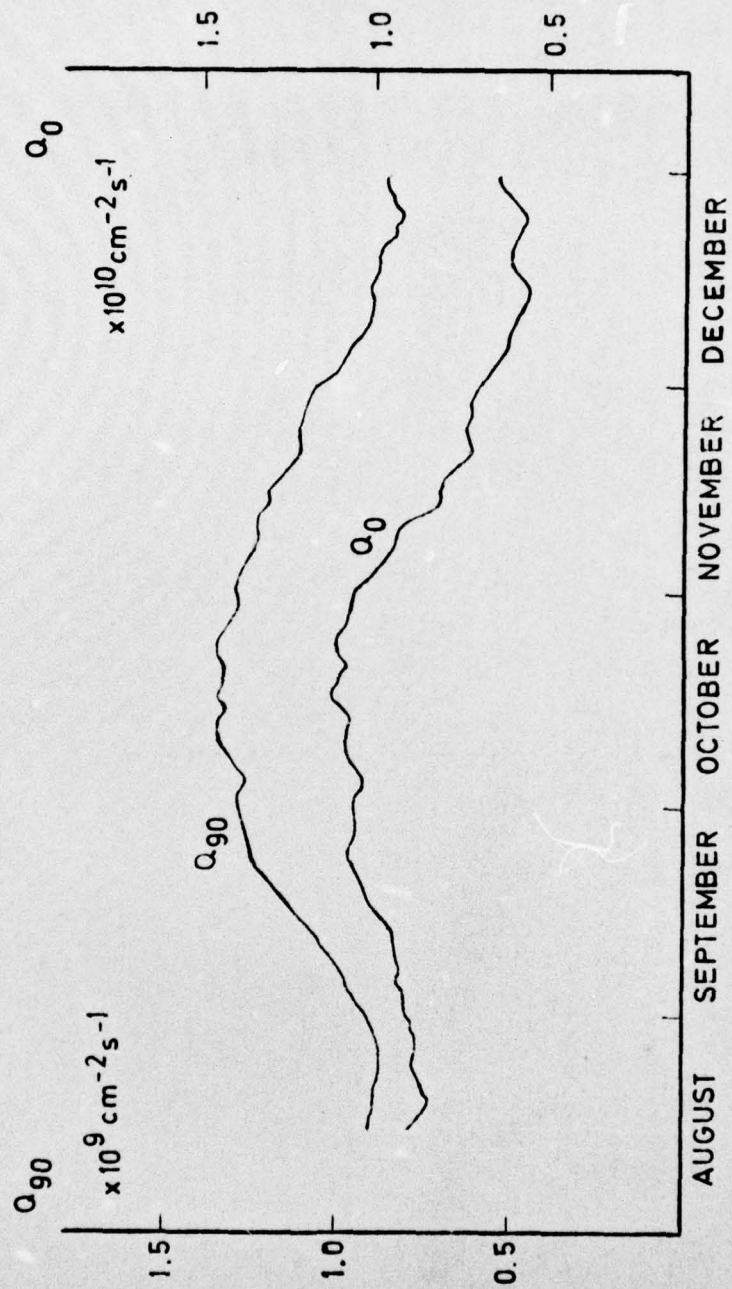


fig. 11. - Running mean of the Q_{90} and Q_0 values obtained by two different procedures

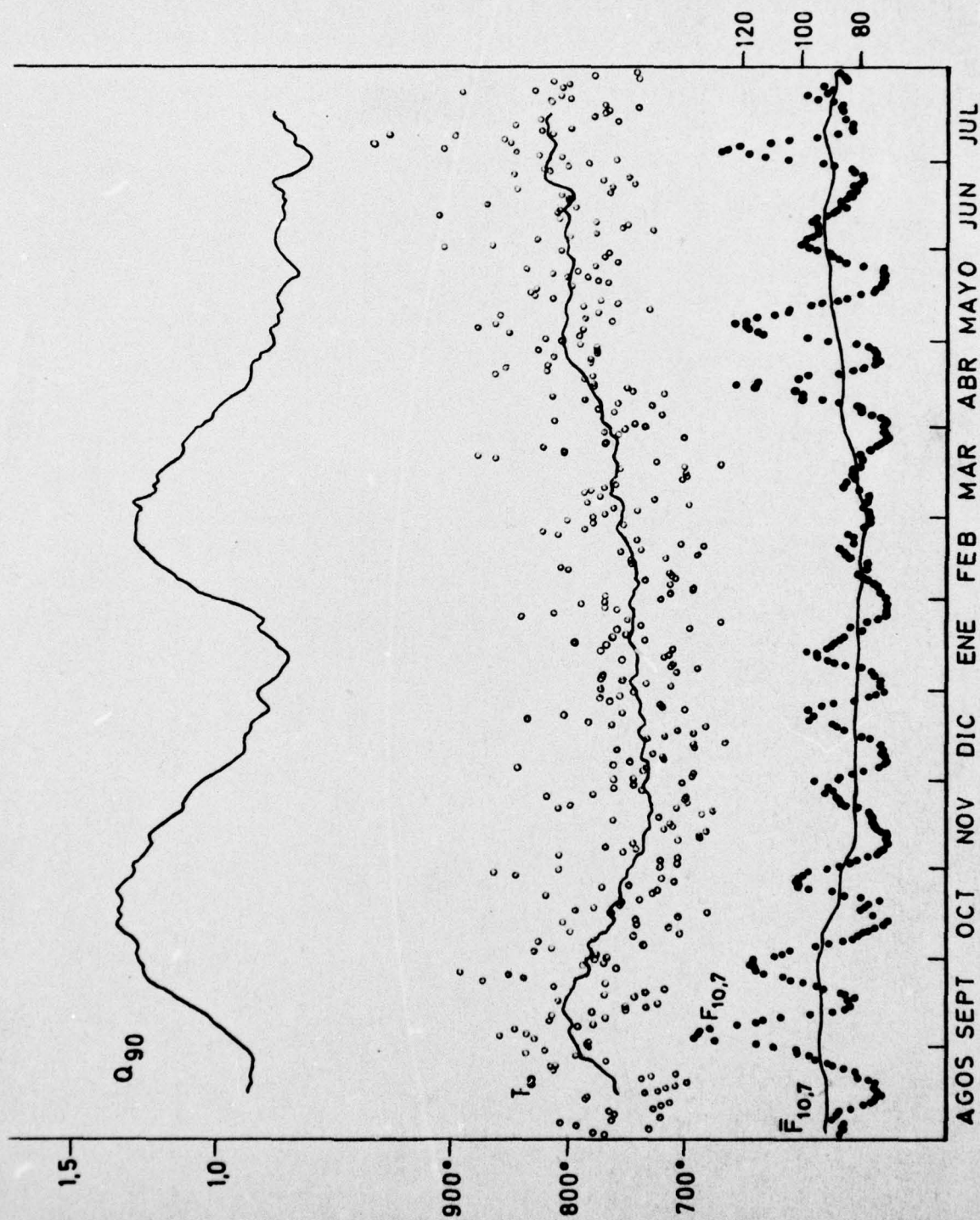


fig. 12. - Variation of Q_{90} , ΔT_{90} , T_{90} and $F_{10.7}$ between August 1973 and July 1974

ces are so small that no conclusion can be drawn from them. But what seems clear is that neither the solar flux nor the exospheric temperature show a seasonal variation that can explain the kind of semiannual variation of the Q_{90} values.

It seems that we are left with the only explanation that the shape of the Q_{90} curve should be attributed to changes in the atmospheric composition, with an increase of the $[O] / [N_2]$ concentration relation in the maxima of the curve.

The experimental data of atmospheric composition seems to agree with such variations with maxima in equinoxes and minima in summer and winter (Mayr and Mahajan (1971), Von Zahn (1972), Jacchia (1974)). As mentioned in a previous report (Alberca and Galdón, 1974) the annual variation can be caused by transport of atomic oxygen from the summer to the winter hemisphere caused by the heating of the atmosphere of the summer hemisphere. The semiannual variation can be produced by a similar mechanism, with a heating source in the auroral zones, that produces a displacement of air rich in atomic oxygen towards lower latitudes (Mayr and Volland 1971 and 1972). This heating source can be related to the semiannual variation of geomagnetic activity. In fact, Strickland and Thomas (1976) have found evidence of transport of O from high to low latitudes, at high altitudes, during magnetic storms, and Pröls and Fricke (1976) have deduced, from data of ESRO 4, enhancement of the N_2 density in regions of high and middle latitudes during periods of increasing magnetic activity.

An increase of the $[O] / [N_2]$ relation, shall also produce an increase in the density of ionization. Now, in the Observatorio del Ebro, the maxima of the total electron content, always have been found at equi

noxes (Galdón 1968, Galdón and Alberca(1970)) and, with the exception of a year of very high solar activity, the summer values have always been higher than the winter ones. Such results seems to support, the idea that the small winter anomaly of the values of Q_{90} may not be significant. We may also notice that, from the stations analyzed by Koster, only Auckland has a semiannual variation of Q bigger than the annual one (as is the case of Ebro), and it is also the station that do not present winter anomaly in the values of the total electron content, another similarity with Ebro.

The results of Titheridge (1974) suggest a latitudinal variation of the amplitude of the annual and semiannual variation of Q . The results of Ebro seem to confirm this suggestions as far as the semiannual variation is concerned, but do not agree for the annual one. Nevertheless, it is to be noticed the great difference of longitude between the stations analyzed by Titheridge and the Observatorio del Ebro. If there is a longitudinal variation of Q_{90} , it is still possible that a latitudinal dependence of the amplitude of the annual variation could be compatible with the Ebro results.

4. CONCLUSIONS.

A method has been developed to obtain daily values of the integrated ionization rate of the atomic oxygen, Q_{90} , from total electron content data. The method has been applied to the data recorded at the Observatorio del Ebro during the period August 1973-July 1974 and daily values of Q_{90} for this pe-

riod have been obtained.

The mean value of them is $Q_{90} = 1.0 \cdot 10^9 \text{ cm}^2 \text{ s}^{-1}$ and the daily values show a semiannual variation with maxima on October and on February-March and minima on January (the sharpest one) and on summer. The October maximum is slightly higher than the February-March one and the minimum of summer is slightly lower than the winter one.

The difference between the two maxima could be due to a variation of the solar activity that, during the analyzed period shows a minimum in February and March. To the same cause could be attributed the difference between the Q_{90} values of August and January. However, the differences in both, the solar activity and the Q_{90} values, are too small to draw final conclusions.

An harmonic analysis of the Q_{90} values gives a first harmonic of 15% amplitude of the mean value, with maximum on December the 1st and minimum on June the 1st. The amplitude of the second harmonic is 20% with maxima on September the 28th and March the 29th-30th, and minima on December the 28th and June 29th.

These temporal variations of Q_{90} , seems to be caused by changes in atmospheric composition, since cannot be explained by parallel variation of other geophysical parameters. These variations indicate an increase of the concentration relation $[O] / [N_2]$ in the maxima of the Q_{90} curve.

The comparison with results of other authors agrees with a latitudinal variation of the mean value of Q_{90} , with maximum towards the equator and also with the Q_{90} variation with the solar activity.

Data from more stations at different latitudes are

needed to establish a latitudinal dependence (if any) of the Q_{90} seasonal variations. With the few data we have, it may be said tentatively that, at middle latitudes, the amplitude of the semiannual variation increases with latitude. On the other hand, the results of Ebro taken in conjunction with the results of other stations, do not seem to support the idea of a regular latitudinal dependence of the annual variation, unless there is also a longitudinal effect.

APPENDIX

PARAMETER OF THE ATMOSPHERIC MODEL.

The lower limit has been fixed to a haight of $z_0 = 120$ Km. and the data at this level are indicated by the subindex 0.

If T_∞ is the exospheric temperature, the temperature profile with height is given by

$$T = T_\infty - (T_\infty - T_0) e^{-b(z-z_0)} \quad (A-1)$$

and the numerical density of the j component by (cfr. 2.2 for its deduction

$$n_j = n_{j0} \left[\frac{T_0}{T} \right]^{\gamma_j} e^{-\frac{1}{H_{mj}}(z-z_0)} (1 + k_j(z-z_0) e^{S_j(z-z_0)}) \quad (A-2)$$

where

$$H_{mj} = (K T_\infty) / (m_j C) \quad \text{and} \quad \gamma_j = 1 + 1 / (b H_{mj})$$

with K = Boltzman constant and m_j molecular weight of the j element.

From the six parameters of (A-1) and (A-2), one is constant, another two depend only on T_∞ and the other three are function of T_∞ and m_j . The value of T_∞ is obtained by the method given by Jacchia (1971).

The formulae for its obtention are :

$$C = 910$$

$$b = 0,028 - T_{\infty} 10^{-5}$$

$$T_0 = 212,4 + T_{\infty} (0,20994 - 0,6 10^{-4} (T_{\infty} - 1))$$

$$s_j = (8,42 + T_{\infty} (2,75 10^{-6} (T_{\infty} - 1) - 7,52225 10^{-3}) + \\ + (m_j/16 - 1)(4,822 + T_{\infty} (2,2985 10^{-6} (T_{\infty} - 1) - 5,0127 10^{-3}) - \\ - 0,5 10^{-9} (T_{\infty} - 1)^3) 10^{-3}$$

$$k_j =$$

$$\text{for the O : } (1,25 + 1,5 10^{-4} T_{\infty}) 10^{-4}$$

$$\text{ " " N}_2 : (0,83 + T_{\infty} (2,505 10^{-14} + 0,5 10^{-6} (T_{\infty} - 1))) 10^{-4}$$

$$\text{ " " O}_2 : (-8,76 + T_{\infty} (3,41375 10^{-2} - 3,9154 10^{-5} (T_{\infty} - 1)) + \\ + (1/3) 4,6 10^{-8} (T_{\infty} - 1)^3) 10^{-4}$$

$$\log n_{j_0} =$$

$$\text{for the O : } 11,1212 - T_{\infty} (1,75088 10^{-4} - 2,4465 10^{-7} (T_{\infty} - 1)) - \\ - (7/6) 10^{-10} (T_{\infty} - 1)^3$$

$$\text{ " " N}_2 : 11,0755 + T_{\infty} (1,16895 10^{-3} - 1,2137 10^{-6} (T_{\infty} - 1)) + \\ + (13/3) 10^{-10} (T_{\infty} - 1)^3$$

$$\text{ " " O}_2 : 10,1168 + T_{\infty} (1,45949 10^{-3} - 1,51335 10^{-6} (T_{\infty} - 1)) + \\ + 5,5 10^{-10} (T_{\infty} - 1)^3$$

The temperatures are given in degrees Kelvin, the heights in Km and the densities in particles per cm³.

M = 32 T(INF) = 700.0°K

Z	T	LOG N JAC	LOG N	β
150	503.0	9.3170	9.3164	- 0
160	540.3	8.9952	8.9947	- 0
180	595.1	8.4263	8.4199	- 2
200	631.1	7.9099	7.9014	- 2
220	654.7	7.4222	7.4156	- 2
240	670.2	6.9530	6.9502	- 1
260	680.4	6.4966	6.4978	0
280	687.2	6.0496	6.0542	1
300	691.6	5.6098	5.6163	2
320	694.5	5.1757	5.1840	2
340	696.4	4.7463	4.7548	2
360	697.6	4.3210	4.3287	2
380	698.4	3.8993	3.9054	2
400	699.0	3.4809	3.4849	1
420	699.3	3.0654	3.0672	1
440	699.6	2.6529	2.6524	- 0
460	699.7	2.2431	2.2405	- 1
480	699.8	1.8360	1.8316	- 1
500	699.9	1.4314	1.4259	- 1
520	699.9	1.0293	1.0234	- 1
540	700.0	0.6297	0.6240	- 1
560	700.0	0.2325	0.2279	- 1

M = 28 T(INF) = 700.0°K

Z	T	LOG N JAC	LOG N	%
150	503.0	10.3149	10.3146	- 0
160	540.3	10.0291	10.0292	- 0
180	595.1	9.5265	9.5213	- 1
200	631.1	9.0718	9.0646	- 2
220	654.7	8.6433	8.6378	- 1
240	670.2	8.2315	8.2295	- 1
260	680.4	7.8312	7.8330	- 1
280	687.2	7.4394	7.4446	- 1
300	691.6	7.0540	7.0616	- 2
320	694.5	6.6738	6.6827	- 2
340	696.4	6.2977	6.3070	- 2
360	697.6	5.9253	5.9340	- 2
380	698.4	5.5560	5.5634	- 2
400	699.0	5.1896	5.1951	- 1
420	699.3	4.8258	4.8290	- 1
440	699.6	4.4647	4.4653	- 0
460	699.7	4.1059	4.1040	- 1
480	699.8	3.7494	3.7452	- 1
500	699.9	3.3952	3.3890	- 2
520	699.9	3.0432	3.0354	- 2
540	700.0	2.6933	2.6845	- 2
560	700.0	2.3456	2.3364	- 2
580	700.0	1.9999	1.9909	- 2
600	700.0	1.6562	1.6481	- 2
620	700.0	1.3146	1.3078	- 2
640	700.0	0.9750	0.9700	- 1
660	700.0	0.6373	0.6345	- 1
680	700.0	0.3016	0.3011	- 0

M = 16

T(INF) = 700.0°K

Z	T	LOG N JAC	LOG H	δ
150	503.0	10.3490	10.3534	1
160	540.3	10.1721	10.1773	1
180	595.1	9.8692	9.8698	0
200	631.1	9.6007	9.5986	- 1
220	654.7	9.3505	9.3487	- 1
240	670.2	9.1117	9.1118	0
260	680.4	8.8806	8.8832	1
280	687.2	8.6551	8.6603	1
300	691.6	8.4339	8.4410	2
320	694.5	8.2159	8.2245	2
340	696.4	8.0005	8.0100	2
360	697.6	7.7874	7.7972	2
380	698.4	7.5761	7.5856	2
400	699.0	7.3667	7.3753	2
420	699.3	7.1588	7.1662	2
440	699.6	6.9523	6.9582	1
460	699.7	6.7473	6.7514	1
480	699.8	6.5437	6.5458	1
500	699.9	6.3413	6.3415	0
520	699.9	6.1402	6.1384	- 1
540	700.0	5.9403	5.9367	- 1
560	700.0	5.7417	5.7363	- 1
580	700.0	5.5442	5.5374	- 2
600	700.0	5.3479	5.3399	- 2
620	700.0	5.1528	5.1438	- 2
640	700.0	4.9588	4.9493	- 2
660	700.0	4.7659	4.7562	- 2
680	700.0	4.5742	4.5646	- 2
700	700.0	4.3836	4.3744	- 2
720	700.0	4.1940	4.1857	- 2
740	700.0	4.0055	3.9983	- 2
760	700.0	3.8181	3.8122	- 1
780	700.0	3.6318	3.6274	- 1
800	700.0	3.4464	3.4439	- 1
820	700.0	3.2622	3.2614	- 0
840	700.0	3.0790	3.0800	0
860	700.0	2.8967	2.8996	1
880	700.0	2.7155	2.7201	1
900	700.0	2.5353	2.5415	2
920	700.0	2.3561	2.3636	2
940	700.0	2.1779	2.1865	2
960	700.0	2.0006	2.0100	2
980	700.0	1.8243	1.8340	2
1000	700.0	1.6490	1.6586	2
1050	700.0	1.2149	1.2220	2
1100	700.0	0.7865	0.7875	0
1150	700.0	0.3639	0.3546	- 2

M = 32

T(INF) = 800.0°K

Z	T	LOG M JAC	LOG M	β
150	548.7	9.3798	9.3743	- 1
160	594.2	9.0775	9.0745	- 1
180	662.1	8.5527	8.5464	- 2
200	707.5	8.0844	8.0765	- 2
220	738.0	7.6471	7.6407	- 2
240	758.5	7.2294	7.2262	- 1
260	772.2	6.8252	6.8256	0
280	781.3	6.4307	6.4342	1
300	787.5	6.0435	6.0493	1
320	791.6	5.6620	5.6693	2
340	794.4	5.2850	5.2930	2
360	796.2	4.9119	4.9197	2
380	797.5	4.5422	4.5492	2
400	798.3	4.1755	4.1813	1
420	798.9	3.8116	3.8158	1
440	799.2	3.4503	3.4527	1
460	799.5	3.0915	3.0923	0
480	799.7	2.7350	2.7344	- 0
500	799.8	2.3808	2.3792	- 0
520	799.9	2.0289	2.0267	- 1
540	799.9	1.6791	1.6770	- 1
560	799.9	1.3314	1.3300	- 0
580	800.0	0.9858	0.9856	- 0
600	800.0	0.6423	0.6439	0
620	800.0	0.3008	0.3047	1

M = 28

T(INF) = 800.0°K

Z	T	LOG N JAC	LOG N	%
150	548.7	10.3656	10.3601	- 1
160	594.2	10.0964	10.0935	- 1
180	662.1	9.6315	9.6257	- 1
200	707.5	9.2185	9.2111	- 2
220	738.0	8.8338	8.8277	- 1
240	758.5	8.4669	8.4637	- 1
260	772.2	8.1122	8.1123	0
280	781.3	7.7662	7.7694	1
300	787.5	7.4268	7.4323	1
320	791.6	7.0925	7.0995	2
340	794.4	6.7623	6.7699	2
360	796.2	6.4356	6.4431	2
380	797.5	6.1118	6.1186	2
400	798.3	5.7907	5.7962	1
420	798.9	5.4721	5.4758	1
440	799.2	5.1557	5.1575	1
460	799.5	4.8415	4.8413	- 0
480	799.7	4.5294	4.5272	- 1
500	799.8	4.2193	4.2152	- 1
520	799.9	3.9112	3.9055	- 1
540	799.9	3.6049	3.5982	- 2
560	799.9	3.3006	3.2931	- 2
580	800.0	2.9980	2.9903	- 2
600	800.0	2.6973	2.6898	- 2
620	800.0	2.3983	2.3916	- 2
640	800.0	2.1011	2.0955	- 1
660	800.0	1.8056	1.8016	- 1
680	800.0	1.5118	1.5096	- 1
700	800.0	1.2197	1.2195	- 0
720	800.0	0.9293	0.9311	1
740	800.0	0.6405	0.6443	1
760	800.0	0.3533	0.3589	1
780	800.0	0.0678	0.0749	2

M = 16

T(INF) = 800.0°K

Z	T	LOG N JAC	LOG N	%
150	548.7	10.3633	10.3647	0
160	594.2	10.1939	10.1978	1
180	662.1	9.9099	9.9110	0
200	707.5	9.6635	9.6624	- 0
220	738.0	9.4372	9.4361	- 0
240	758.5	9.2234	9.2237	0
260	772.2	9.0178	9.0203	1
280	781.3	8.8183	8.8228	1
300	787.5	8.6230	8.6294	2
320	791.6	8.4311	8.4389	2
340	794.4	8.2418	8.2505	2
360	796.2	8.0547	8.0638	2
380	797.5	7.8694	7.8784	2
400	798.3	7.6858	7.6943	2
420	798.9	7.5036	7.5112	2
440	799.2	7.3227	7.3291	2
460	799.5	7.1432	7.1480	1
480	799.7	6.9648	6.9681	1
500	799.8	6.7876	6.7891	0
520	799.9	6.6116	6.6113	- 0
540	799.9	6.4366	6.4345	- 1
560	799.9	6.2628	6.2590	- 1
580	800.0	6.0899	6.0846	- 1
600	800.0	5.9181	5.9114	- 2
620	800.0	5.7474	5.7395	- 2
640	800.0	5.5776	5.5689	- 2
660	800.0	5.4088	5.3996	- 2
680	800.0	5.2410	5.2315	- 2
700	800.0	5.0741	5.0647	- 2
720	800.0	4.9083	4.8991	- 2
740	800.0	4.7433	4.7348	- 2
760	800.0	4.5793	4.5717	- 2
780	800.0	4.4162	4.4097	- 2
800	800.0	4.2541	4.2489	- 1
820	800.0	4.0929	4.0891	- 1
840	800.0	3.9325	3.9304	- 1
860	800.0	3.7731	3.7726	- 0
880	800.0	3.6145	3.6158	0
900	800.0	3.4568	3.4598	1
920	800.0	3.3000	3.3046	1
940	800.0	3.1440	3.1502	2
960	800.0	2.9889	2.9964	2
980	800.0	2.8347	2.8433	2
1000	800.0	2.6813	2.6907	2
1050	800.0	2.3014	2.3115	2
1100	800.0	1.9266	1.9348	2
1150	800.0	1.5568	1.5600	1
1200	800.0	1.1919	1.1866	- 1
1250	800.0	0.8318	0.8142	- 4
1300	800.0	0.4764	0.4425	- 8
1350	800.0	0.1256	0.0711	- 12

- 53 -

M = 32

T(INF) = 900.0°K

Z	T	LOG N JAC	LOG N	%
150	590.6	9.4282	9.4184	- 2
160	644.1	9.1402	9.1353	- 1
180	725.0	8.6478	8.6425	- 1
200	780.3	8.2156	8.2095	- 1
220	818.2	7.8166	7.8117	- 1
240	844.0	7.4385	7.4360	- 1
260	861.7	7.0746	7.0748	0
280	873.8	6.7207	6.7233	1
300	882.1	6.3742	6.3787	1
320	887.8	6.0334	6.0391	1
340	891.6	5.6971	5.7033	2
360	894.3	5.3646	5.3707	2
380	896.1	5.0353	5.0406	1
400	897.3	4.7089	4.7130	1
420	898.2	4.3850	4.3877	1
440	898.8	4.0635	4.0645	0
460	899.2	3.7443	3.7435	- 0
480	899.4	3.4272	3.4248	- 1
500	899.6	3.1122	3.1083	- 1
520	899.6	2.7992	2.7942	- 1
540	899.8	2.4882	2.4824	- 1
560	899.9	2.1790	2.1729	- 2
580	899.9	1.8718	1.8657	- 1
600	900.0	1.5663	1.5609	- 1
620	900.0	1.2627	1.2583	- 1
640	900.0	0.9609	0.9579	- 1
660	900.0	0.6608	0.6596	- 0
680	900.0	0.3625	0.3631	0
700	900.0	0.0659	0.0685	1

M = 28

T(INF) = 900.0°K

Z	T	LOG N JAC	LOG N	%
150	590.6	10.4044	10.3940	- 2
160	644.1	10.1473	10.1417	- 1
180	725.0	9.7100	9.7043	- 1
200	780.3	9.3282	9.3217	- 2
220	818.2	8.9767	8.9713	- 1
240	844.0	8.6442	8.6412	- 1
260	861.7	8.3246	8.3242	- 0
280	873.8	8.0141	8.0161	1
300	882.1	7.7103	7.7143	1
320	887.8	7.4116	7.4170	1
340	891.6	7.1170	7.1232	2
360	894.3	6.8257	6.8321	2
380	896.1	6.5373	6.5433	1
400	897.3	6.2514	6.2566	1
420	898.2	5.9678	5.9717	1
440	898.8	5.6863	5.6888	1
460	899.2	5.4068	5.4076	0
480	899.4	5.1292	5.1284	- 0
500	899.6	4.8534	4.8510	- 1
520	899.7	4.5794	4.5756	- 1
540	899.8	4.3070	4.3021	- 1
560	899.9	4.0364	4.0306	- 1
580	899.9	3.7674	3.7612	- 2
600	900.0	3.5000	3.4937	- 2
620	900.0	3.2342	3.2282	- 1
640	900.0	2.9699	2.9646	- 1
660	900.0	2.7072	2.7029	- 1
680	900.0	2.4460	2.4430	- 1
700	900.0	2.1963	2.1848	- 3
720	900.0	1.9282	1.9282	- 0
740	900.0	1.6714	1.6731	0
760	900.0	1.4162	1.4195	1
780	900.0	1.1624	1.1671	1
800	900.0	0.9100	0.9158	1
820	900.0	0.6591	0.6657	2
840	900.0	0.4095	0.4165	2
860	900.0	0.1613	0.1681	2

M = 16

T(INF) = 900.0 °K

Z	T	LOG N JAC	LOG N	
150	590.6	10.3735	10.3723	- 0
160	644.1	10.2092	10.2122	1
180	725.0	9.9384	9.9409	1
200	780.3	9.7082	9.7091	0
220	818.2	9.4998	9.5007	0
240	844.0	9.3048	9.3068	1
260	861.7	9.1188	9.1224	1
280	873.8	8.9391	8.9443	1
300	882.1	8.7640	8.7706	2
320	887.8	8.5923	8.6001	2
340	891.6	8.4232	8.4318	2
360	894.3	8.2563	8.2653	2
380	896.1	8.0911	8.1002	2
400	897.3	7.9275	7.9362	2
420	898.2	7.7653	7.7733	2
440	898.8	7.6043	7.6114	2
460	899.2	7.4446	7.4504	1
480	899.4	7.2859	7.2903	1
500	899.6	7.1283	7.1311	1
520	899.7	6.9717	6.9730	0
540	899.8	6.8161	6.8157	- 0
560	899.9	6.6615	6.6595	- 1
580	899.9	6.5073	6.5043	- 1
600	900.0	6.3551	6.3502	- 1
620	900.0	6.2032	6.1971	- 2
640	900.0	6.0523	6.0451	- 2
660	900.0	5.9022	5.8943	- 2
680	900.0	5.7530	5.7445	- 2
700	900.0	5.6047	5.5959	- 2
720	900.0	5.4573	5.4484	- 2
740	900.0	5.3106	5.3020	- 2
760	900.0	5.1648	5.1566	- 2
780	900.0	5.0199	5.0124	- 2
800	900.0	4.8757	4.8691	- 2
820	900.0	4.7324	4.7269	- 1
840	900.0	4.5899	4.5857	- 1
860	900.0	4.4481	4.4454	- 1
880	900.0	4.3072	4.3059	- 0
900	900.0	4.1670	4.1673	0
920	900.0	4.0276	4.0295	1
940	900.0	3.8889	3.8925	1
960	900.0	3.7510	3.7561	1
980	900.0	3.6139	3.6204	2
1000	900.0	3.4776	3.4852	2
1100	900.0	2.8067	2.8172	3
1200	900.0	2.1536	2.1580	1
1300	900.0	1.5176	1.5039	- 3
1400	900.0	0.8980	0.8523	- 10
1500	900.0	0.2942	0.2018	- 19

- 56 -

M = 32

T(INF) = 1000.0 °K

Z	T	Log N JAC	LOG N	%
150	628.5	9.4666	9.4542	- 3
160	689.7	9.1893	9.1841	- 1
180	783.5	8.7215	8.7187	- 1
200	848.9	8.3172	8.3143	- 1
220	894.6	7.9481	7.9461	- 1
240	926.5	7.6012	7.6006	- 0
260	948.7	7.2691	7.2702	0
280	964.2	6.9474	6.9502	1
300	975.0	6.6334	6.6374	1
320	982.6	6.3251	6.3300	1
340	987.9	6.0213	6.0266	1
360	991.5	5.7212	5.7264	1
380	994.1	5.4242	5.4289	1
400	995.9	5.1299	5.1337	1
420	997.1	4.8380	4.8407	1
440	998.0	4.5484	4.5498	0
460	998.6	4.2609	4.2608	- 0
480	999.0	3.9753	3.9738	- 0
500	999.3	3.6917	3.6889	- 1
520	999.5	3.4099	3.4060	- 1
540	999.7	3.1298	3.1251	- 1
560	999.8	2.8515	2.8462	- 1
580	999.8	2.5749	2.5695	- 1
600	999.9	2.2999	2.2947	- 1
620	999.9	2.0266	2.0219	- 1
640	1000.0	1.7549	1.7511	- 1
660	1000.0	1.4848	1.4821	- 1
680	1000.0	1.2163	1.2149	- 0
700	1000.0	0.9493	0.9494	0
720	1000.0	0.6838	0.6855	0
740	1000.0	0.4199	0.4230	1
760	1000.0	0.1575	0.1619	1

M = 28

T(INF) = 1000.0°K

Z	T	LOG N JAC	LOG N	β
150	628.5	10.4352	10.4207	- 3
160	689.7	10.1869	10.1794	- 2
180	783.5	9.7705	9.7655	- 1
200	848.9	9.4126	9.4075	- 1
220	894.6	9.0869	9.0827	- 1
240	926.5	8.7815	8.7788	- 1
260	948.7	8.4896	8.4887	- 0
280	964.2	8.2072	8.2081	0
300	975.0	7.9318	7.9341	1
320	982.6	7.6615	7.6649	1
340	987.9	7.3955	7.3994	1
360	991.5	7.1323	7.1367	1
380	994.1	6.8722	6.8764	1
400	995.9	6.6144	6.6181	1
420	997.1	6.3588	6.3617	1
440	998.0	6.1052	6.1071	1
460	998.6	5.8535	5.8541	0
480	999.0	5.6034	5.6029	- 0
500	999.3	5.3551	5.3533	- 1
520	999.5	5.1083	5.1055	- 1
540	999.7	4.8631	4.8593	- 1
560	999.8	4.6195	4.6150	- 1
580	999.8	4.3773	4.3724	- 1
600	999.9	4.1366	4.1315	- 1
620	999.9	3.8973	3.8924	- 1
640	1000.0	3.6595	3.6550	- 1
660	1000.0	3.4230	3.4193	- 1
680	1000.0	3.1879	3.1851	- 1
700	1000.0	2.9542	2.9526	- 0
720	1000.0	2.7218	2.7215	- 0
740	1000.0	2.4907	2.4919	0
760	1000.0	2.2609	2.2635	1
780	1000.0	2.0325	2.0364	1
800	1000.0	1.8053	1.8104	1
820	1000.0	1.5795	1.5855	1
840	1000.0	1.3549	1.3615	2
860	1000.0	1.1315	1.1384	2
880	1000.0	0.9094	0.9161	2
900	1000.0	0.6885	0.6944	1
920	1000.0	0.4688	0.4734	1
940	1000.0	0.2503	0.2529	1
960	1000.0	0.0331	0.0329	- 0

- 58 -

M = 16 T(INF) = 1000.0 °K

Z	T	LOG N JAC	LOG N	%
150	628.5	10.3811	10.3762	- 1
160	689.7	10.2204	10.2213	0
180	783.5	9.9589	9.9615	1
200	848.9	9.7407	9.7425	1
220	894.6	9.5460	9.5477	0
240	926.5	9.3657	9.3680	1
260	948.7	9.1951	9.1983	1
280	964.2	9.0311	9.0354	1
300	975.0	8.8719	8.8772	1
320	982.6	8.7162	8.7223	2
340	987.9	8.5632	8.5699	2
360	991.5	8.4124	8.4193	2
380	994.1	8.2633	8.2703	2
400	995.9	8.1158	8.1224	2
420	997.1	7.9695	7.9757	2
440	998.0	7.8245	7.8298	1
460	998.6	7.6805	7.6848	1
480	999.0	7.5376	7.5407	1
500	999.3	7.3956	7.3975	1
520	999.5	7.2546	7.2551	0
540	999.7	7.1145	7.1136	- 0
560	999.8	6.9753	6.9730	- 1
580	999.8	6.8370	6.8332	- 1
600	999.9	6.6994	6.6944	- 1
620	999.9	6.5627	6.5566	- 2
640	1000.0	6.4269	6.4197	- 2
660	1000.0	6.2918	6.2838	- 2
680	1000.0	6.1575	6.1489	- 2
700	1000.0	6.0240	6.0149	- 2
720	1000.0	5.8912	5.8820	- 2
740	1000.0	5.7593	5.7501	- 2
760	1000.0	5.6280	5.6192	- 2
780	1000.0	5.4976	5.4892	- 2
800	1000.0	5.3678	5.3602	- 2
820	1000.0	5.2388	5.2321	- 2
840	1000.0	5.1105	5.1049	- 1
860	1000.0	4.9829	4.9786	- 1
880	1000.0	4.8561	4.8532	- 1
900	1000.0	4.7299	4.7285	- 0
920	1000.0	4.6044	4.6046	0
940	1000.0	4.4797	4.4815	1
960	1000.0	4.3556	4.3590	1
980	1000.0	4.2321	4.2372	1
1000	1000.0	4.1094	4.1160	2
1100	1000.0	3.5056	3.5178	3
1200	1000.0	2.9179	2.9293	3
1300	1000.0	2.3454	2.3468	0
1400	1000.0	1.7878	1.7676	- 5
1500	1000.0	1.2444	1.1899	- 12

BIBLIOGRAPHY

- Alberca, L.F. and E.Galdón(1974): Some results of electron content measurements at Tortosa from the INTELSAT II-F3 transmissions Sc.Rep.Nº5. Observatorio del Ebro.
- CIRA (1965):COSPAR International reference atmosphere 1965. Compiled by the membres of COSPAR working group IV, North-Holland Publ. C. Amsterdam, 313 pg.
- Chapman, S.(1931): The absorption and dissociative or ionizing effect of monochromatic radiation in an atmosphere on a rotating earth. Part.II.Grazing incidence. Proc. Phys. Soc. 43, 483-501.
- Galdón, E.(1968): Daily and seasonal variation of the total electron content of the ionosphere over Tortosa. J.S.S.G. Rep. nº 3 Add. 84-107.
- Galdón, E. and L.F.Alberca(1970): Influence of solar activity on the total electron content of the ionosphere over Tortosa. Rad. Sci. 5, 913-915.
- Garriot, O.K. and F.L. Smith(1965): The rate production of electrons in the ionosphere.Planet.Space. Sci. 13, 839-849.
- Jacchia,L.G.(1970): New static models of the thermosphere and exosphere with empirical temperature profiles. Smith. Astr.Obs. Special Rep. 313.
- Jacchia,L.G.(1971): Revised static models of the thermosphere and exosphere with empirical temperature profiles. Smithsonian Astrophysical Obs. Special Rep. 332.
- Jacchia, L.G.(1974): Variations in thermospheric composition: A model based on mass spectrometer and satellite drag data. J. Geophys. Res. 79, 1923-1927.

- Kockarts, G. (1973): Heat balance and thermal conduction. Physics and Chemistry of upper atmospheres. Ed. B. M. McCormac. D. Reidel Pub. Co. Dordrecht-Holland, pp. 54-63.
- Koster, J. R. (1976): Ionospheric production rates and the initial zenith angle at Legon. J. Atmos. Terr. Phys. 38, 611-114.
- Majid, A. and M. V. Bhuriwala (1976): Total electron content measurements at Karachi. Ann. Geophys. 32, 57-62.
- Mayr, H. G. and K. K. Mahajan (1971): Seasonal variations in the F2 region. J. Geophys. Res. 76, 1017-1028.
- Mayr, H. G. and H. Volland (1971): Semiannual variation in the neutral composition. Ann. Geophys. 27, 513-522.
- Mayr, H. G. and H. Volland (1972): Theoretical model for the latitude dependence of the thermospheric annual and semiannual variations. J. Geophys. Res. 77, 6774-6790.
- Narcisi, R. S. (1973): Mass spectrometer measurements in the ionosphere. Physics and Chemistry of upper atmospheres. Ed. B. M. McCormac. D. Reidel Pub. Co. Dordrecht-Holland pp. 171-183.
- Pröls, G. W. and K. H. Fricke (1976): Neutral composition changes during a period of increasing magnetic activity. Planet. Space Sci. 24, 61-67.
- Rao, N. N. (1967): Ionospheric content and irregularities deduced from BE-C satellite transmissions. J. Geophys. 72, 2929-2942.
- Risbeth, H. and C. S. G. K. Setty (1961): The F-layer at sunrise. J. Atmos. Terr. Phys. 20, 263-276.
- Smith, F. L. III (1968): Determination of rates of production and loss of electrons in the F-region of the ionosphere from observations of geostationary satellite transmissions. Tech. Rep. n°10. Stanford Electronic Laboratory

ries, Stanford University.

Spurling, P.H. (1972): Dependence of calculated integrated production rates on solar activity. *J. Atm. Terr. Phys.* 34, 1151-1152.

Strickland, D.J. and G.E. Thomas (1976): Global atomic oxygen density derived from OGO-6 1304 Å airglow measurements. *Planet. Space Sci.* 24, 313-326.

Taylor, G.N. (1965): Integrated electron production and loss rates in the ionosphere. *Planet. Space Sci.* 13, 507.

Titheridge, J.E. (1966): Continuous records of the total electron content of the ionosphere. *J. Atm. Terr. Phys.* 28, 1138-1150.

Titheridge, J.E. (1974): Changes in atmospheric composition from ionospheric production rates. *J. Atm. Terr. Phys.* 36, 1249-1257.

Tyagi, T.R. and A.P. Mitra (1970): Some geographic and geophysical aspects of electron content measurements from satellite radio beacon transmissions. *J. Atm. Terr. Phys.* 32, 1807-1818.

Von Zahn, U. (1972): Neutral air density and composition. *Physics and Chemistry of upper atmospheres*. D. Reidel Pub. Co. Ed. B.M. Cormac, p. 3-10.

Whitten, R.C. and I.G. Poppoff (1974): Fundamentals of aeronomy. John Wiley and Sons, Inc. New York, 446 pp.

Yeh, K.C., B.J. Flaherty and H.R. Cho (1969): Studies of the ionosphere at geomagnetically conjugate stations, Ionosphere Radio Lab. Dep. of Electrical En. University of Illinois. Final Report.

Unclassified

SECURITY CLASSIFICATION OF THIS PAGE (When Data Entered)

REPORT DOCUMENTATION PAGE

READ INSTRUCTIONS
BEFORE COMPLETING FORM

1. REPORT NUMBER

2. GOVT ACCESSION NO.

Scientific rept. no. 6 (Final),
Aug 73-Jul 74,

3. TITLE (and Subtitle)

IONOSPHERIC ELECTRON PRODUCTION RATE
FOR GRAZING INCIDENCE AT THE EBRO
OBSERVATORY

4. TYPE OF REPORT & PERIOD COVERED
Final Report

5. PERFORMING ORG. REPORT NUMBER

6. AUTHOR(s)

L. F. Alberca/s. I.

7. CONTRACT OR GRANT NUMBER(s)

AFOSR-75-2745

8. PERFORMING ORGANIZATION NAME AND ADDRESS

Observatorio Del Ebro
Apartado 9
Tortosa, Spain

9. PROGRAM ELEMENT, PROJECT, TASK
AREA & WORK UNIT NUMBERS

62101F

46430101

10. CONTROLLING OFFICE NAME AND ADDRESS

Air Force Geophysics Laboratory
Hanscom AFB, Massachusetts 01731
Monitor/John P. Mullen/PHP

11. REPORT DATE

29 Dec 77

12. MONITORING AGENCY NAME & ADDRESS (if different from Controlling Office)

13. NUMBER OF PAGES

65

14. SECURITY CLASS. (of this report)

Unclassified

15. DECLASSIFICATION/DOWNGRADING
SCHEDULE

16. DISTRIBUTION STATEMENT (of this Report)

Approved for public release; distribution unlimited.

17. DISTRIBUTION STATEMENT (of the abstract entered in Block 20, if different from Report)

18. SUPPLEMENTARY NOTES

19. KEY WORDS (Continue on reverse side if necessary and identify by block number)

Total electron content
Electron production rate

20. ABSTRACT (Continue on reverse side if necessary and identify by block number)

Values of total electron content of the ionosphere, obtained at the Observatorio del Ebro by the Faraday rotation method, have been analyzed to study electron production rates. Daily values of the electron production rate, integrated with respect to height through the ionosphere, were determined at sunrise for the period August 1973-July 1974, by a method that makes use of a two components model atmosphere. A Fourier analysis of the results indicates an annual and a semiannual variation of the production

Unclassified

SECURITY CLASSIFICATION OF THIS PAGE (When Data Entered)

rat values. A comparison with results of other authors seems to indicate a latitudinal dependence of the semiannual variation; no similar effect was found for the annual variation.



Unclassified

SECURITY CLASSIFICATION OF THIS PAGE (When Data Entered)